# CONTROL OF A SPACECRAFT USING MIXED MOMENTUM EXCHANGE DEVICES

A Thesis

presented to

the Faculty of California Polytechnic State University,

San Luis Obispo

In Partial Fulfillment

of the Requirements for the Degree

Master of Science in Aerospace Engineering

By

Blake Currie

October 2014

COMMITTEE MEMBERSHIP

| | |
|---|---|
| TITLE: | Control of a Spacecraft Using Mixed Momentum Exchange Devices |
| AUTHOR: | Blake Currie |
| DATE SUBMITTED: | October 2014 |
| COMMITTEE CHAIR: | Eric Mehiel, Associate Professor<br>Aerospace Engineering Department |
| COMMITTEE MEMBER: | Jordi Puig-Suari, Professor<br>Aerospace Engineering Department |
| COMMITTEE MEMBER: | Kira Abercromby, Assistant Professor<br>Aerospace Engineering Department |
| COMMITTEE MEMBER: | Colleen Kirk, Professor<br>Department of Mathematics |

ABSTRACT

Control of a Spacecraft Using Mixed Momentum Exchange Devices

Blake Currie

Hardware configurations, a control law, and a steering law are developed for a mixed hardware spacecraft that uses both control moment gyros and reaction wheels. Replacing one or more gyros in a spacecraft with a reaction wheel has potential for cost savings while still achieving much greater performance than using reaction wheels alone. Several simulated tests are run to compare the performance to a traditional all reaction wheel or all control moment gyro spacecraft, including analysis of failure modes and singular configurations. The mixed system performed similarly to all gyro systems, responding within 6% of the gyro system's time for all nominal cases. It far exceeds the performance of reaction wheel systems, taking only a fourth of the time. It also handles failures better than reduced size gyro systems. As such, it can be an effective cost saving measure for certain satellite missions.

# TABLE OF CONTENTS

# LIST OF TABLES

# LIST OF FIGURES

# 1. Introduction

Many spacecraft missions require fine attitude control. While thrusters and electromagnetic torque rods provide external torques, precision control is usually achieved using momentum exchange devices (MEDs). The devices are capable of spinning freely, and when their angular momentum is changed, the angular momentum of the spacecraft must also change to conserve net angular momentum. They consume no fuel, but do not provide external torque, and so must be supported by thrusters or torque rods. Two common MEDs exist: control moment gyros (CMGs) and reaction wheels.

## 1.1 Momentum Exchange Devices

Reaction wheels are quite simple, and consist of a motor and a wheel. The motor changes the wheel's momentum by increasing or decreasing the spin rate. In reaction, the spacecraft is torqued in the opposite direction. CMGs use an additional mechanism to alter its angular momentum. The same motor and wheel assembly are used, but the spin rate remains constant. Instead, the spin axis is changed using a gimbal and an additional motor. Changing the spin axis changes the direction of the CMG's angular momentum vector, and again the spacecraft's angular momentum changes to conserve the net angular momentum vector. A simple diagram of a CMG, showing the spin and gimbal axes, can be found in figure 1.

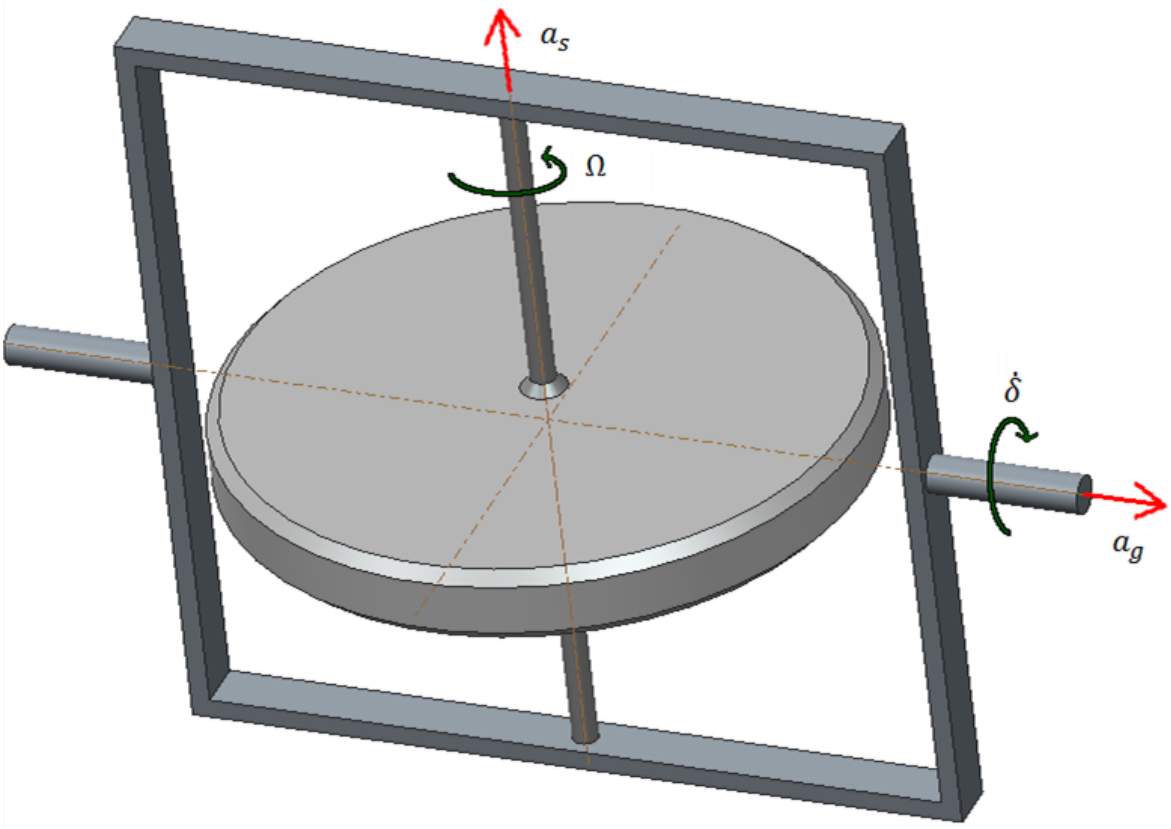


**Figure 1. A simple CMG.** The wheel spins at a constant rate Ω about the spin axis $a_s$. The direction of the spin axis changes based on the gimbal angle δ around the gimbal axis $a_g$. Torque is produced by inducing a gimbal rate $\dot{\delta}$.

CMGs and reaction wheels each have their own advantages. The reaction wheel is much simpler in terms of hardware. As a result, reaction wheels tend to be less expensive and have a longer life than CMGs. They usually have lower mass, volume, and power usage as well. In addition, reaction wheels are much easier to implement.[1,2] While reaction wheels produce torque in a constant direction, the torque magnitude and direction changes in a CMG based on the gimbal angle. As a result, a set of CMGs may encounter singularities – configurations in which torque cannot be produced in a particular direction. A

steering law, which distributes torque amongst the devices, may help to avoid singularities. However, it does not work in all cases and may introduce error into the system.[3]

Despite these disadvantages, CMGs remain very important. This is because CMGs take advantage of torque amplification. While reaction wheel output torque is limited by the motor's torque, a CMG may output several times the torque placed on the gimbal.[3] As a result, CMGs can output much larger amounts of torque and so may maneuver a spacecraft much more quickly than reaction wheels alone. In combination, reaction wheels and maneuvering thrusters are also capable of providing high torque and accuracy. However, this is best suited for satellites which only slew occasionally.[4] Otherwise, the resulting fuel usage becomes too costly and sometimes completely prohibitive. In these cases, CMGs are needed.

### 1.2 Thesis Purpose

The purpose of this thesis is to establish a control scheme that uses both reaction wheels and CMGs in tandem. This includes selecting a hardware configuration, establishing a control law, and implementing a steering law that incorporates both types of MEDs. While the control law decides how much torque should be output to the spacecraft, the steering law decides how to divide the torque amongst the devices and is key to ensuring that a mixed system functions correctly.

Despite similar usage and operation, CMGs are rarely if ever used in combination with reaction wheels. However, certain missions may not require a full set of CMGs. In one case, the spacecraft may require more torque than reaction wheels can provide, but do not require the full torque capability of a CMG set. In another case, a particular axis may not require high torque even if others do. For example, the roll orientation of a camera may not be important, so long as the axis is stable and the orientation is known. In both of these cases, at least one CMG could be replaced with a reaction wheel.

If at least one CMG could be replaced with a reaction wheel, some cost and mass would be saved. For example, for the same maximum angular momentum output, a Honeywell M-50 CMG has a mass of 24kg, while the constellation series reaction wheel has a mass of 8.5kg.[5,6] Since CMGs typically have a shorter on-orbit lifetime, reducing the number of CMGs reduces the likelihood of a failure. Additionally, if the reaction wheel is included in the steering law, the reaction wheel eliminates the possibility of singularity in the direction of the wheel's torque vector. As a result, singularities are less likely to occur and unless the reaction wheel is allowed to saturate, singularities may only occur within a plane rather than in any direction.

For a more specific example, take the SPOT satellites. The SPOT satellites produce high resolution ground imaging. The recently launched SPOT-6 and SPOT-7 satellites upgraded to using CMGs, whereas previous SPOT missions had used reaction wheels. The benefits of this upgrade can be seen in

figure 2.[7] With CMGs, the SPOT satellite is able to take more pictures when alternating pictures across the ground track.

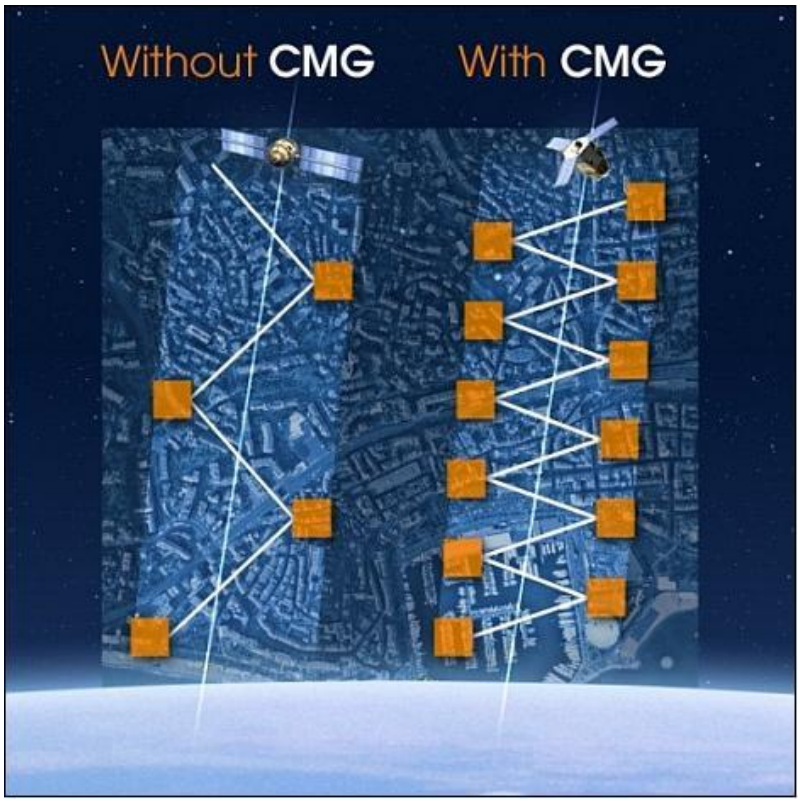


**Figure 2. SPOT mission CMG comparison.** With CMGs, it is possible to get a higher density of pictures along the ground track. (Image credit: Astrium SAS)[7]

In figure 2, the movement along the ground track is caused by the movement of the satellite, but the faster slewing of the CMGs allows the camera to move to either side of the ground track more quickly, so that more of these alternating pictures can be taken. This mission would potentially be an excellent candidate for a mixed system. In this case, agility is only needed in one axis, in the cross-track direction. The camera roll axis does not change, and the in-track

direction rotates at a constant rate to face the earth, but requires no torque. In this case, one or even two of the CMGs could be replaced with reaction wheels and the satellite could still experience similar performance with the correct hardware configuration.

In particular, this thesis will focus on establishing the performance of a system with three CMGs and a single reaction wheel. Additionally, while double gimbal CMGs exist, this thesis only examines single gimbal CMGs.

# 2. Background Research

While most research focuses on CMGs or reaction wheels alone, some research on mixed control systems does exist. Quite a bit of research has also been performed on variable speed control moment gyros (VSCMGs). And while research on mixed systems of CMGs and reaction wheels is limited, research has been done on several other mixed control system combinations.

## 2.1 MED Combined Control

In one paper, Skelton examines a control scheme for a satellite with three CMGs and three reaction wheels.[8] However, the control schemes in Skelton's research use the CMGs and reaction wheels for different purposes. While this thesis looks to reduce the cost of an actuator system while keeping the benefits of both, Skelton aims to use the reaction wheels primarily for stabilization, and the CMGs primarily for rapid slewing. In one control scheme, the CMGs are run with open loop control, and the reaction wheels are used to correct for errors. In another, parallel control laws are used for the CMGs and reaction wheels, but they are never implemented together.

Another paper by Roithmayr proposes a mixed control scheme for the international space station.[9] However, this proposal is at a scale far beyond those of normal satellites. Roithmayr proposes using 48 pairs of reaction wheels, with each pair operating in opposite directions. This allows the reaction wheels to be used both for control purposes and for energy storage. These reaction wheels would be used in tandem with the double gimbal CMGs currently aboard the

international space station. The control law for this also separates the CMGs and reaction wheels, and is based on reducing a cost function rather than using classical control techniques.

There has also been much research recently on variable speed control moment gyros (VSCMGs). In a VSCMG, the speed of the wheel on the gimbal may also be varied. This allows each device to be used both as a reaction wheel and as a CMG. This additional degree of freedom allows each device to perform singularity escape on its own, or even store power.[3] Although at least one prototype has been made[10], VSCMGs remain largely experimental. Additionally, they are even more complex in terms of both hardware and control software implementation, have higher power requirements, and induce vibrations.[11] Using the device as a CMG shifts the torque axis of the reaction wheel usage, and using the device as a reaction wheel increases or decreases the torque output by the CMG usage. A VSCMG system is quite similar in concept to the mixed system proposed here. However, since singularities are less of a concern, VSCMG steering laws tend to focus on either storing power or preventing wheel speeds (and therefore gimbal torque output) from becoming too low.[3] As a result, the same steering laws cannot be used.

### 2.2 Other Mixed Control Systems

More literature can be found on combined control with other actuators. Particularly common are control schemes that utilize both reaction thrusters and reaction wheels.[4,12,13] Since MEDs require an actuator that can provide external

torque anyway, satellites that use reaction wheels often have thrusters as well. The high torque provided by the thrusters is complimented by the high accuracy but low torque of the reaction wheels. As mentioned previously, this may be ideal for some missions, but for others fuel costs are prohibitive. Due to the bang-bang control strategy of thrusters and the problem of singularities in CMG, mixed control strategies are very different between a thruster-wheel system and a CMG-wheel system. Since CMGs are not involved, these mixed systems also do not need to address singularities.

Another combined control system is described by Lappas for CMGs and electromagnetic torque rods (ETRs). This combination has many similarities to a mixed CMG and reaction wheel system. However, in this paper, the ETRs were used as a way to reject external torques and keep the gimbal angles in an ideal range prior to slewing. The ETRs were not used within the steering law to directly aid in singularity escape.[14]

### 2.3 Steering Laws

The steering law, in its most basic form, decides how to distribute torque amongst multiple devices. The torque output is calculated by multiplying a 3xN matrix by an Nx1 control input vector, where N is the number of devices that may be selected. Therefore, inverting the matrix and multiplying by a desired torque will give the required control inputs to achieve the desired torque. If there are only three devices and no singularities, the matrix is square and may be inverted. A more general solution uses the Moore-Penrose pseudo inverse. With CMGs

however, the Moore-Penrose solution tends to encounter singular states and provides no method to escape them.[15] As a result, there are many steering laws targeted specifically for CMGs. While the Moore-Penrose pseudo inverse solves the system in a least squares sense, other CMG steering laws solve the system such that singular states are avoided or escaped.

In order to develop a steering law for a mixed control system, many steering laws were considered for a basis. Reaction wheel steering laws are generally very simple, using the pseudo inverse to distribute momentum in a least squares fashion. Since the torque direction is fixed, there is no risk of the matrix become singular. However, it is possible to incorporate reaction wheels within many more complex CMG steering laws. As a result, a CMG steering law was chosen as a basis to work from.

Several CMG steering laws were considered before one was chosen. Initially, a steering law which used linear programming was considered. Because of its use of cost functions, it would be fairly easy to add in reaction wheels and even other actuators all into a single control scheme. It already incorporated thrusters into its CMG steering law. This was done by charging a high cost for thrusters such that they were only used if the maneuver could not be completed without them[16] Ultimately this approach was abandoned in favor of more modern approaches that are more commonly used. This would allow the mixed control to be more easily implemented and updated for modern systems.

A hybrid steering law was also considered. There are generally two main types of CMG steering laws. The first is called singular avoidance, which uses

null motion to minimize some measure of the singularity. This approach does not introduce any error into the system, but it cannot avoid certain types of singularities.[15] The second type of steering law is called singular escape. In singular escape, a small error is introduced in the system when a singularity is approached. Although the introduction of error can delay the system's response, it can escape more types of singularities than the singular avoidance methods.

The hybrid approach detects the type of singularity as it is approaching, and uses the singular escape, singular avoidance, or both methods. Having the ability to use both, in avoids introducing error when possible, but can still deal with the broader range of singularity types. This is a very recent and modern approach.[15] However, for a first attempt at a mixed control steering law, it was decided that only one type of law should be used in order to make the testing easier. If the system doesn't work as expected, the error could be caused by either steering law or by the mechanics that tie them together.

The addition of the reaction wheel does provide some interesting implications for both types of steering laws. In singular avoidance methods, the reaction wheel allows the CMGs to use the reaction wheel to assist in null motion. In singular escape methods, the reaction wheel reduces the amount of error that needs to be added. In both cases, this assists with singularities that have a component in the reaction wheel spin axis, since it can absorb angular momentum without changing the torque direction.

Finally, a steering law known as singular direction avoidance, developed by Ford and Hall[17], was chosen as the basis. Though called singular direction

avoidance, it is actually a singular escape method. This is one of the base steering laws used in the recently developed hybrid steering law and so still seems to be in use. It uses singular value decomposition in order to determine which direction a singularity may occur in, and how close it is to occurring. If the CMGs approach a singular configuration, the steering law introduces an error in the singular direction so that the matrix remains invertible, although as a result the output will not be exactly as commanded. However, since it only introduces error in the singular direction, the output error is relatively small.[17] A more detailed description of this steering law is contained in the next section.

# 3. Analysis

In this section, the governing equations for momentum exchange devices (MEDs) will be derived. Then a summary of the singular direction avoidance method will be presented. Finally, an explanation of the modifications to the singular direction avoidance will be given.

## 3.1 Governing Equations for MEDs

The total angular momentum of a spacecraft can be found as the sum of the momentum of its parts. The spacecraft momentum vector *h* is:

$$\vec{h} = J\,\vec{\omega} + A_g I_{cg}\dot{\delta} + A_s I_{ws}\Omega \qquad (1)$$

The first term is the angular momentum of the spacecraft body, with J being the spacecraft moment of inertia including all reaction wheels and CMGs, and $\omega$ being the spacecraft body's rotation vector. The second term includes gimbal rotation momentum. $A_g$ is a matrix with columns that are the MED gimbal axis vectors. $I_{cg}$ is the moment of inertia of the gimbal and the wheel about the gimbal axis, and $\dot{\delta}$ is the gimbal rate. The final term accounts for the momentum of the spinning wheels. $A_s$ is a matrix with columns that are the MED spin axis vectors. $I_{ws}$ is the moment of inertia of the wheel, and Ω is the wheel rotation rate.

In order to find the resulting control torque given wheel speed changes and gimbal rates, we must take the derivative of the above equation. To take the

derivative, it is important to note what is constant and what is changing. As the control inputs, the gimbal rates ($\dot{\delta}$ ) and wheel speeds (Ω) will change. As the output we are looking to change, the spacecraft rotation rate (ω) will not be constant either. The gimbal axes ($A_g$) are constant, but the spin axes ($A_s$) are dependent on the gimbal angle and will change. The moment of inertia of the wheel and gimbal ($I_{cg}$ and $I_{ws}$) are constant within the gimbal frame and may be considered constant. However, the overall moment of inertia of the spacecraft (J) will change as the gimbal axes move. As a result, the derivative of the spacecraft angular momentum vector is:

$$\dot{\vec{h}} = \dot{J}\,\vec{\omega} + J\,\dot{\vec{\omega}} + A_g I_{cg}\ddot{\delta} + \dot{A}_s I_{ws}\Omega + A_s I_{ws}\dot{\Omega} \tag{2}$$

To calculate the derivative the spin axis orientation matrix, it is important also to know the torque axis vector. The torque axis is perpendicular to both the spin and gimbal axes, and is found by taking the cross product of the gimbal and torque vectors. It is also the instantaneous direction of the torque output by a positive gimbal rate. When the gimbal angles are all at zero, the resulting torque and spin axis vectors are denoted by a subscript 0 ($A_{s0}$ and $A_{t0}$). To determine the rate of change of $A_s$, we first relate the spin axes to the gimbal angles. Relative to the gimbal angle, the spin and torque axes are:

$$A_s(\delta) = A_{s0}\,[cos(\delta)]^D + A_{t0}\,[\sin(\delta)]^D \tag{3}$$

$$A_t(\delta) = A_{t0}\,[cos(\delta)]^D - A_{s0}\,[\sin(\delta)]^D \tag{4}$$

The superscript D represents a diagonalized matrix of the values in the vector. Taking the derivative, we can pull out $\dot{\delta}$ from all terms, resulting in:

$$\dot{A}_s = (-A_{s0}\,[sin(\delta)]^D + A_{t0}\,[\cos(\delta)]^D)\,[\dot{\delta}]^D = A_t[\dot{\delta}]^D \quad (5)$$

$$\dot{A}_t = (-A_{t0}\,[sin(\delta)]^D - A_{s0}\,[\cos(\delta)]^D)\,[\dot{\delta}]^D = -A_s[\dot{\delta}]^D \quad (6)$$

The total spacecraft moment of inertia can be broken down into four terms. The first term is the spacecraft body's moment of inertia without the MEDs. The other terms account for the moment of inertia of the MEDs in each axis.

$$J = I_B + A_s I_{cs} A_s^T + A_t I_{ct} A_t^T + A_g I_{cg} A_g^T \quad (7)$$

In taking the derivative, the moment of inertia of the spacecraft is constant in the body frame, as is the gimbal moment of inertia since the gimbal axis is fixed. Taking the derivative of the remaining terms,

$$\dot{J} = \dot{A}_s I_{cs} A_s^T + A_s I_{cs} \dot{A}_s^T + \dot{A}_t I_{ct} A_t^T + A_t I_{ct} \dot{A}_t^T \quad (8)$$

Substituting in the equations (3, 4) and simplifying:

$$\dot{J} = A_t[\dot{\delta}]^D (I_{cs} - I_{ct}) A_s^T + A_s[\dot{\delta}]^D (I_{cs} - I_{ct}) A_t^T \quad (9)$$

Finally, the change in angular momentum vector can be related back to the angular rate of the spacecraft such that:

$$\dot{\vec{h}} = \omega^{\times}\vec{h} = w^{\times}\left(J\,\vec{\omega} + A_g I_{cg}\dot{\delta} + A_s I_{ws}\Omega\right) \tag{10}$$

where the superscript x indicates the skew symmetric form of the vector. Substituting equations 5, 9 and 10 into equation 2, and collecting like terms:

$$\begin{gathered}\left[A_t\left[\dot{\delta}\right]^D(I_{cs} - I_{ct})A_s^T + A_s\left[\dot{\delta}\right]^D(I_{cs} - I_{ct})A_t^T\right]\vec{\omega} \;+\; J\dot{\vec{\omega}} \;+ \\ A_t I_{ws}[\Omega]^D\dot{\delta} \;+\; A_g I_{cg}\ddot{\delta} \;+\; A_s I_{ws}\dot{\Omega} \;+\; \vec{\omega}^{\times}\left(J\vec{\omega} + A_g I_{cg}\dot{\delta} + A_s I_{ws}\Omega\right) \;=\; 0\end{gathered} \tag{11}$$

Equation 11 forms the equations of motion for any type of momentum exchange device. CMGs and reaction wheels may use simplified versions of this equation. For reaction wheels, gimbal rate and acceleration are a constant zero, and the gimbal angle is constant and is considered zero for simplicity. For CMGs, wheel spin rate is constant and wheel spin acceleration is zero. Even using CMGs, the gimbal acceleration term is also often ignored as it is usually small relative to the other terms.

### 3.2 CMG Control

From there, we can group terms that have command inputs (wheel speed and acceleration or gimbal speed and acceleration) which act as the output torque of the device. The remaining terms have the body rate or acceleration

terms, which constitute the spacecraft's reaction to the torque. For reaction wheels, this process is fairly simple, as all the spin rate terms can easily be grouped. However, the gimbal rate terms are not as easy to combine because the gimbal rate is in the middle of each term, and they cannot be simply removed because of matrix multiplication. In order to separate the control inputs for a CMG, the control law is added first. The exact derivation depends on the control law used, but it is generally of the form:

$$A_g I_{cg} \ddot{\delta} + D\dot{\delta} = L_r \tag{12}$$

In Ford and Hall, the following control law is used:

$$L_r = K(\omega - \omega_f) + kG(q_f)^T q - J\dot{\omega}_f + h^{\times}\omega + g_e \tag{13}$$

where $L_r$ is the control torque request, k and K are control gains, and q is the attitude quaternion. The subscript f indicates the desired final state, and $g_e$ is an estimation of all external torques on the system. Finally,

$$G(q) = \begin{bmatrix} -q_1 & -q_2 & -q_3 \\ q_0 & -q_3 & q_2 \\ q_3 & q_0 & -q_1 \\ -q_2 & q_1 & q_0 \end{bmatrix} \tag{14}$$

The Ford and Hall paper contains a Lyapunov stability proof of this control law.[17] In Ford and Hall, the D term in equation 12 becomes:

$$D = A_t I_{ws}[\Omega]^D + \frac{1}{2}(A_s A_t^T + A_t A_s^T)(\omega + \omega_f)(I_{ct} + I_{cs}) \quad (15)$$

However, the largest contributor to D is the first term. Therefore, if we ignore the other terms, D is simply:

$$D = A_t I_{ws}[\Omega]^D \quad (16)$$

In Ford and Hall, the other terms were seven orders of magnitude smaller than the remaining term.[17] However, the unsimplified D expression can be used for high accuracy testing and applications or for setups that may be more sensitive to the ignored terms. If we also ignore the gimbal acceleration, then for a three CMG setup in a nonsingular configuration, the gimbal rates distribution can be found by:

$$\dot{\delta} = D^{-1} L_r \quad (17)$$

However, in most cases there will be more than three actuators and even if there are only three CMGs, singularity protection is desirable. This necessitates the use of a steering law.

### 3.3 Singular Direction Avoidance Steering Law

As mentioned previously, the mixed steering law used in this thesis is based off of a CMG steering law called singular direction avoidance. The method uses singular value decomposition to estimate the closeness to singularity, and will introduce an error when necessary to prevent the system from reaching singularity.

In singular value decomposition, an *m* by *n* matrix D of any size may be broken down into the product of the three matrices such that:

$$D = USV^T \tag{18}$$

U and V are calculated by taking the eigenvectors of $DD^T$ and $D^TD$, respectively. S is calculated as the square root of the eigenvalues of $DD^T$ or $D^TD$, arranged along the diagonal of an *m* by *n* matrix. U and V are unitary matrices that are *m* by *m* and *n* by *n*, respectively. If D is not a square matrix, any additional rows or columns with no diagonal are zero. These zero eigenvalues show up in either $D^TD$ if there are more columns than rows or or $DD^T$ if there are more rows than columns.

In singular value decomposition, the diagonal elements of S are the singular values of the matrix D. If a value of the S matrix approaches zero, the D matrix is approaching a singularity, where the matrix is not full rank and becomes noninvertible. The S matrix is arranged so that the values are sorted from highest to lowest along the diagonal. To find a pseudo-inverse of the matrix D,

$$D^{\dagger} = V_t S_t^{-1} U^T \tag{19}$$

where $V_t$ and $S_t$ are the truncated V and S matrices, where the additional zero rows or columns are removed. For a square matrix, no truncation is required and the inverse is a true inverse. The truncation ensures that the matrix is always square. However, without any modification, S is still not invertible if the matrix D is singular.

This version of the pseudo inverse is used in equation 17 for the singular direction avoidance steering law. However, it is modified slightly to ensure that the matrix can still be inverted even when singular conditions are encountered. Because the maximum diagonal length of the S matrix is 3 (operating in 3 dimensions), the third value will always be the closest to singularity. Unless the CMGs become singular in two dimensions (not possible in pyramid configurations – to be discussed in section 3.5), only the third value needs to be modified in order to prevent the CMGs locking near singularity. Instead of strictly inverting the S matrix, only the first two values are inverted. The third diagonal is instead given the value:

$$S_{33}^{\dagger} = \frac{S_{33}}{S_{33}^2 + \alpha} \tag{20}$$

where $S_{33}^{\dagger}$ is the third diagonal value in the inverted $S_t$ matrix. The alpha term is not constant, but exponentially approaches a fixed value as $S_{33}$ approaches zero.

The rate of this approach can be modified by a gain, and the full error value $\alpha_0$ can also be modified. Since the parameter α is scaled down by the proximity to a singularity, the error introduced is negligible until a singularity is approached.

### 3.4 Steering and Control Law Modification

In order to use the reaction wheel to help accomplish a maneuver and for the reaction wheel to be useful in singularity protection, it must fall under the same steering law as the CMGs. To do so, we refer back to equation 11. Setting gimbal angles, rates, and accelerations to zero, the equations of motion for a reaction wheel can be written as:

$$J\dot{\vec{\omega}} + \vec{\omega}^{\times} J\vec{\omega} + A_s I_{ws}\dot{\Omega} + \vec{\omega}^{\times} A_s I_{ws}\Omega = 0 \tag{21}$$

The first two terms are considered the spacecraft reaction, and the last two terms are the output of the reaction wheel. Therefore, the torque command to a reaction wheel is fulfilled by:

$$L_r = E\dot{\Omega} + \vec{\omega}^{\times} A_s I_{ws}\,\Omega \tag{22}$$

Where:

$$E = A_s I_{ws} \tag{23}$$

However, the steering law can only select one derivative to control. The wheel acceleration is the primary output that we control, so it is selected by the steering

law. The wheel rate on the other hand is not directly commanded and does not respond as quickly. The wheel rate term is less significant, but may still be notable. Instead of ignoring it, it is compensated for in the control law. In this way it is not directly controlled, but does not become an error in the torque output of the system. So, with the CMGs included, the steering law can be formatted in a block matrix form:

$$\begin{bmatrix} \dot{\delta} \\ \dot{\Omega} \end{bmatrix} = \begin{bmatrix} D & E \end{bmatrix}^{\dagger} L_r \tag{24}$$

This same basis is used for controlling VSCMGs as well.[3]

The control law simply finds the torque request $L_r$, so it does not change based on what devices are being used. As such, the control law used in Ford and Hall (eq. 13) works just as well for the mixed system as it does for a four CMG system. However, the control law requires modification for the second proposed setup, in which agility is only needed in two axes. In certain cases, the roll angle about a sensor's axis only needs to be known, not controlled. The problem can't be entirely reduced to two dimensions however, because the roll rate must still be controlled to avoid sensor distortion. This cannot be directly integrated into the Ford and Hall control law because there is no way to isolate the roll angle into the individual quaternion elements. It is possible to convert a Tait-Bryan maneuver (yaw-pitch-roll) with zero roll angle into a quaternion. In this case the roll is commanded to be zero, but this does not allow the roll angle to drift from its initial

position. Allowing the angle to drift somewhat allows for a faster maneuver, so a different control law is used for this purpose.

Instead of the quaternions, a simple proportional control was selected. Torque direction is chosen to be perpendicular to both the current and desired final sensor axis so that a direct path is taken to align the axis. The magnitude is determined linearly by the angle between the axes. This is essentially equivalent to the simplified control law commonly used with simple pendulums in three dimensions. Since only the sensor boresight axis is used for alignment, the roll angle about that axis will not generate any error. However, since the rate control remains unchanged, the roll rate will still converge to zero. The final control law becomes:

$$L_r = K(\omega - \omega_f) + k\theta\hat{u} - J\dot{\omega}_f + h^{\times}\omega + g_e \tag{25}$$

where θ is the angle between the current sensor boresight axis and the final boresight axis. $\hat{u}$ is the unit vector perpendicular to both the current and final boresight axis. It is determined using the cross product. In the event that the desired final axis and current axis are aligned but facing the opposite direction, an arbitrary rotation axis is picked. For this simulation, the rotation axis is picked randomly, but if 180° rotations are anticipated to be encountered, the axis could be picked such that the rotation is in a direction favorable to the current orientation of the CMGs. Doing so would make it less likely to encounter a singularity.

### 3.5 Hardware Layout

In this thesis, two possible hardware configurations are considered. In one case, the purpose is to have performance that is as similar as possible to a four CMG layout, but instead only using three CMGs and a reaction wheel. This is called the symmetric maneuverability layout for future purposes. If the full performance of a four CMG system is not necessary, this can create notable savings in mass and overall cost. Compared to a three CMG system with no reaction wheel, the risk of encountering singularities is much less. Even with singularity avoidance, some singularities cannot be avoided or escaped, and even those that can will introduce an error into the system. This becomes an even bigger problem if a CMG fails in a system with only three devices, at which time there is always a direction in which torque cannot be created.

The second hardware layout to be considered is for a satellite with agility in two axes and stability in the third. In other words, the CMGs are used to quickly point a spacecraft in a particular direction, while the roll rate is kept at zero but roll angle is not commanded. This case is called the two-axis agility layout. In this case, most of the torque from the CMGs is desired to be in a plane perpendicular to the camera or other sensor's roll axis, while the reaction wheel takes most of the control around the sensor axis.

#### 3.5.1 Common CMG Layouts

For systems of four CMGs, there are several common hardware configurations. The first is the rooftop configuration, seen in figure 3 below. In the rooftop configuration, there are two torque planes that meet at an angle. Each

torque plane is occupied by two CMGs. The rooftop configuration does not encounter certain types of singularities by its nature. However, it may encounter a more serious rank 1 singular condition in which the torque axes of all the CMGs are aligned into a single axis, rather than a plane.[11] It would also be difficult to adapt this configuration to a mixed control scheme, since it relies on having two pairs of CMGs.

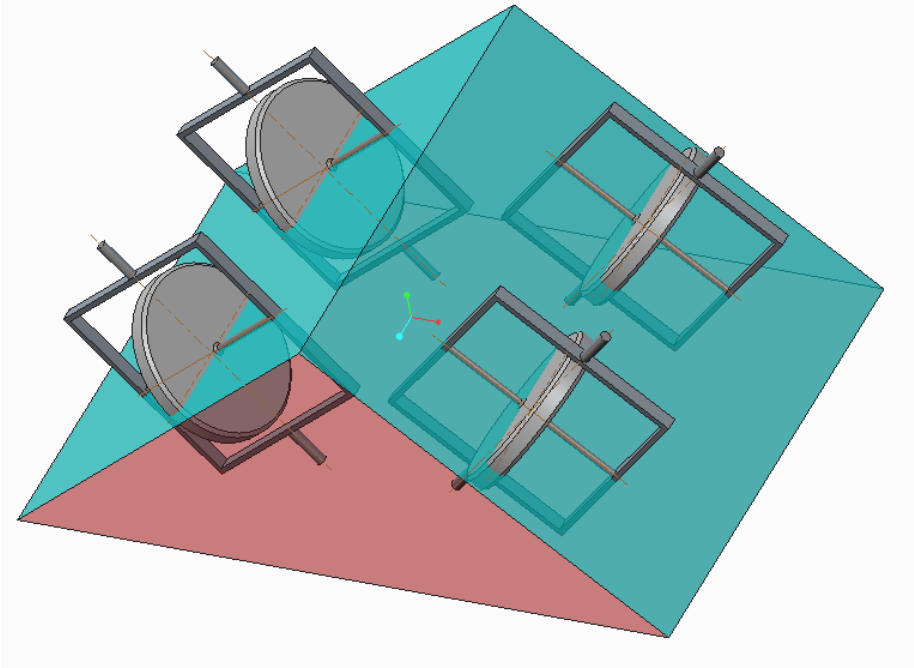

**Figure 3. A rooftop CMG configuration.** Here, there are two CMGs in each torque plane.

The other common layout is a pyramid configuration, seen in figure 4 below. The pyramid configuration creates a symmetrical and near spherical momentum envelope. The momentum envelope represents how much angular momentum can be absorbed in any given direction when the gimbal angles are at zero. Thus, the pyramid configuration is very flexible and can maneuver

quickly in any direction. This is closest to ideal when the pyramid forms half of a regular octahedron, with a pyramid angle of approximately 54.74°. This angle is defined between the base of the pyramid and each face.

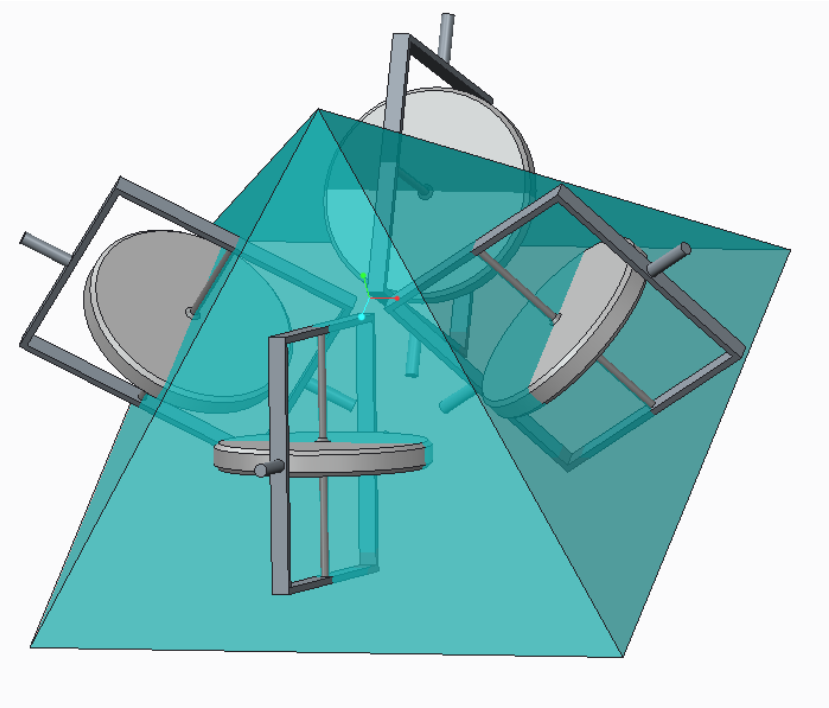

**Figure 4. A pyramid CMG configuration.** The torque planes of the CMGs, which represent all of the possible output torque directions, form a pyramid.

Symmetric, independent CMG configurations are based off of regular polyhedrons. This is done by positioning one CMG perpendicular to all non-parallel surfaces.[18] For example, the common four CMG pyramid is based on half of a regular octahedron. Each half's faces are parallel to the other half's, so only four are placed. An alternate but less used configuration for four CMGs would be to have the CMGs perpendicular to each face of a tetrahedron. And for

configurations with six CMGs, one is placed on each of the six non-parallel surfaces of a dodecahedron. For a three CMG system, this means that the CMGs are mounted on each perpendicular surface of a cube – in other words, all three CMGs are perpendicular. For simplicity, the gimbal axes are generally aligned with the body axes.

### 3.5.2 Symmetric Maneuverability Layout

Adding a reaction wheel significantly complicates the ability to construct a symmetric configuration. The symmetry of regular polyhedrons can be taken advantage of in all-CMG configurations, but since reaction wheels have only a single torque axis rather than two dependent axes, they add differently.

For example, see the momentum envelope for a CMG pyramid versus a reaction wheel pyramid in figure 5. While the reaction wheel pyramid's momentum envelope is a relatively simple geometric figure, the CMG envelope has a smooth curvature. It is also non-convex and overall much more complex, despite being symmetric. Combining elements of both to create a symmetric momentum envelope is not trivial.

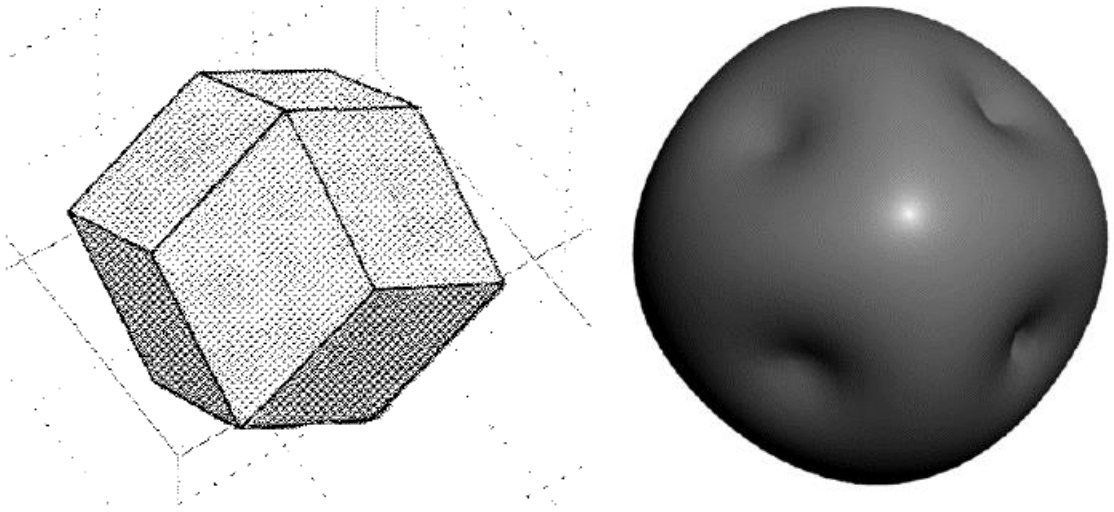

(a) (b)

**Figure 5. Momentum envelope for reaction wheel and CMG pyramids.** The reaction wheel envelope is seen in (a)[19] while the CMG envelope is seen in (b)[20].

For the symmetric maneuverability configuration, the momentum envelope does not actually need to be symmetric. Since the reaction wheel cannot output as much torque as the CMGs, its full momentum capability is not necessarily accessible in the time that a maneuver needs to be completed. As a result, a near spherical momentum envelope would not actually produce equal maneuverability in each direction. So equal momentum capability in each axis is not suitable for the full maneuverability configuration.

Since the reaction wheel produces torque in a constant direction while the CMGs' torque changes direction, it is difficult to analyze what positions will create a symmetric maneuverability. To find a starting point, we can assume that for the purpose of large maneuvers, the reaction wheel torque is negligible. In this case, the three CMGs may all be placed perpendicular to one another, gimbals aligned

with the axes, in the cube configuration discussed earlier. From this initial configuration, the reaction wheel is placed with its spin axis having equal components in each CMG axis. Since the reaction wheel torque is much smaller than the CMG torque, this estimation is reasonably close to ideal. The reaction wheel could still be included by angling the CMG gimbals slightly towards the reaction wheel spin axis. This removes some of the CMGs' torque capability from the direction of the reaction wheel's output torque. However, this angle would be very small and is ignored in later testing. Despite the reaction wheel contributing negligible torque for large maneuvers, it is still useful for singularity avoidance and in the case of CMG failure, as seen in section 4.2.

### 3.5.3 Two Axis Agility Layout

On the other hand, in the case of the two axis agility configuration, symmetric torque output is actually not desired. Instead, it is desirable to have more of the CMG's output torque in the plane perpendicular to the sensor boresight axis. This allows for the opportunity to establish a symmetric (or near symmetric) momentum envelope while still achieving a higher maneuverability in one plane. To start this process, the CMGs are rearranged into a triangular pyramid configuration. This is based on the tetrahedron layout, although the angle will not be the same and there is no CMG in the base of the tetrahedron. The reaction wheel is then set into the vertical axis of the pyramid, as seen in figure 6. Since the reaction wheel has less torque capability, and less torque is needed in the sensor boresight axis, these two axes are aligned.

If the face-edge-face angle is set to $\cos^{-1}\left(\frac{1}{3}\right) \approx 70.53°$, it becomes a tetrahedron, and if the angle is set to $\cos^{-1}\left(\frac{1}{\sqrt{3}}\right) \approx 54.74°$ it becomes a rotation of the cubic system with all three CMGs perpendicular. From 54.74°, increasing the angle increases the torque and momentum available in the vertical axis, while decreasing the angle reduces them in the vertical axis and increases them in the horizontal plane. To create a symmetric envelope after adding the reaction wheel, the angle should be decreased from 54.74°.

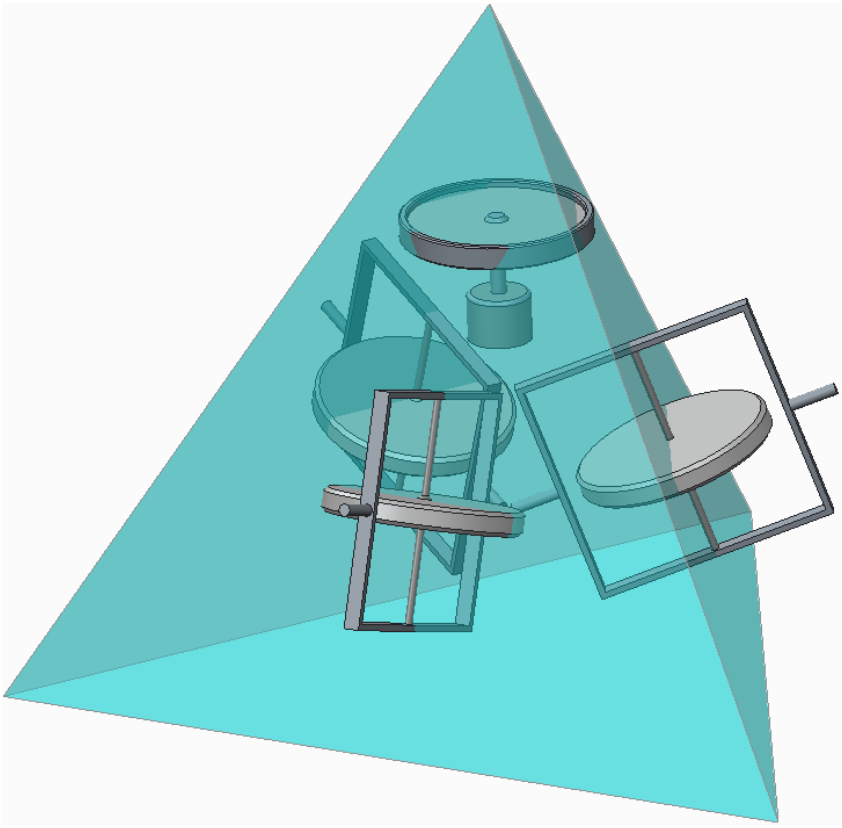

**Figure 6. A tetrahedron CMG configuration with reaction wheel added.** To create a greater torque in the x-y plane and create a more symmetric momentum envelope, the face-edge-face angle is decreased.

The angle should be chosen to produce a symmetric momentum envelope. Luckily, for a single reaction wheel, the addition to the outer momentum envelope is fairly simple. For a reaction wheel in the z (vertical) axis, the reaction wheel's momentum can simply be added in that direction. To clarify, the CMGs have some outer momentum envelope in the horizontal plane – that is when all the momentum is distributed within the horizontal plane. From this, the reaction wheel may add any amount of momentum in either the positive or negative vertical direction until the reaction wheel is saturated. At this point, more momentum can be absorbed in the vertical axis, but only at the cost of decreased momentum in the horizontal plane as the CMGs are shifted. As a result, the momentum envelope appears as a cylinder capped with the CMG momentum envelope.

The maximum vertical momentum can be calculated fairly easily. This is because when the spin axes are as close to vertical as possible, the horizontal components will cancel. In relation to the pyramid angle, the maximum momentum in the vertical direction is:

$$h_z = 3\sin(\theta_p) * h_{CMG} + h_{RW} \tag{26}$$

where $h_z$ is the maximum momentum in the vertical axis, $\theta_p$ is the pyramid angle, $h_{CMG}$ is the momentum of the three CMGs, and $h_{RW}$ is the maximum momentum

of the reaction wheel. If the gimbals are rotated 180° and the reaction wheel is spun up in the opposite direction, the whole quantity becomes negative.

Estimating the maximum momentum in the horizontal xy plane is not quite as simple. Some assumptions will be made here to simplify the process. First, it is assumed that the momentum envelope in the horizontal plane is roughly circular. Next it is assumed that the singular direction is parallel to the momentum vector. This assumption is not always true, particularly near the dimples in the momentum envelope.[20] Both of these assumptions hold fairly well in the horizontal plane for the pyramid configuration, with the horizontal plane being fairly close to an ellipsoid while the dimples are located in the gimbal axis directions .

With these assumptions, we take a singular vector u in the horizontal plane. For each gimbal, the angular momentum vector which produces the singular vector u is calculated as:

$$\vec{h}_n = h_{CMG}\left(\frac{g_n \times u}{\|g_n \times u\|}\right) \times g_n \tag{27}$$

where $g_n$ is the gimbal axis of the $n^{th}$ CMG. The term in parentheses is the unit torque vector perpendicular to the projection of the singular vector. Crossing this again with the gimbal vector produces the singular spin vector, which is scaled by the angular momentum of the CMG. If a singular direction in the y-axis is chosen, the calculation becomes very simple. Not only that, but the singular direction and momentum vectors are parallel as assumed. Substituting the gimbal vectors, a

singular vector in the y direction, and adding the momentums together, the resulting momentum in the y direction is:

$$h_y = h_{CMG}\left(1 + \sqrt{4\cos(\theta_p)^2 + \sin(\theta_p)^2}\right) \quad (28)$$

The one added to the square root term corresponds to the first gimbal, which can point directly in the y direction. Assuming that the angular momentum in the horizontal plane is circular, the pyramid angle corresponding to a roughly symmetric envelope would occur when $h_y$ in equation 28 is set equal to $h_z$ in equation 26. If the reaction wheel and CMGs have the same angular momentum, the resulting pyramid angle is $\cos^{-1}\left(\sqrt{\frac{2}{3}}\right) \approx 35.3°$. This is consistent with the previous assessment that the angle needed to be reduced. To check the symmetry, a model of the momentum envelope was created. This model can be seen below in figure 7.

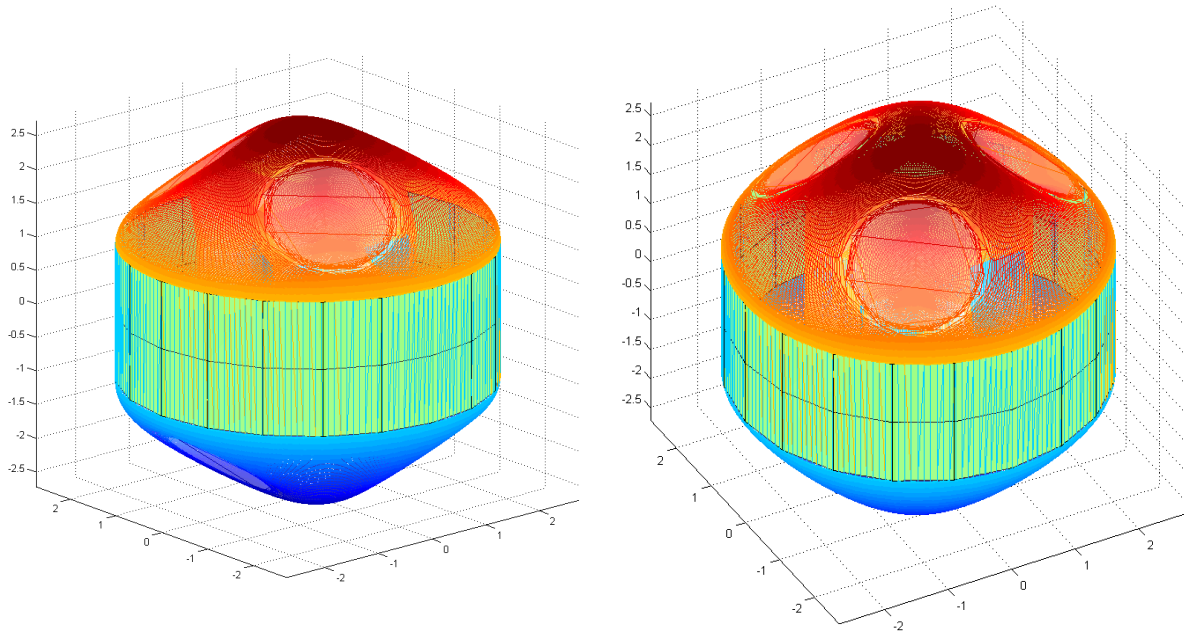

**Figure 7. Two axis agility system momentum envelope.** The two images are different perspectives of the same envelope. The code use to generate the model was adapted from the code used in Leve.[15]

After closely examining the momentum envelope, the figure seems to be fairly symmetrical. The top view confirms the horizontal plane is roughly circular as assumed, and the maximum height of the envelope from the center is equal to the diameter of the cylinder portion.

# 4. Results

In order to check the performance of the system, a computer simulation was created in MATLAB Simulink. The symmetric maneuverability and 2-axis agility configurations were tested for performance and are compared to the performance of an all CMG system and an all reaction wheel system. Failure modes and singularity cases were examined as well.

## 4.1 Simulation Description

In this simulation, it is assumed that there are no external forces acting on the satellite. The hardware configuration and control gains are entered as parameters. An initial and desired final quaternion and angular rate are input as commands. For the two-axis agility configuration, the quaternions are translated into an initial and final desired sensor axis.

In creating the hardware parameters and in designing the simulation, the goal was to be as realistic as possible. The data sheets of the Honeywell M-50 control moment gyro[5] and Constellation Series reaction wheel[6] were used to model the reaction wheels and the control moment gyros. Additionally, all device limitations were checked to ensure they were not exceeded during the simulation. This includes maximum gimbal acceleration, maximum spin rate of the reaction wheel, torque output of the reaction wheels, etc. The satellite itself was not modeled after a particular satellite, but is aimed to match a moderately sized satellite. The fixed parameters used in the simulation can be seen in table 1. These remained constant across all tests.

**Table 1. Fixed simulation parameters.** These parameters stay constant both during each test and across all tests.

| Description | Symbol | Value | Units |
|---|---|---|---|
| Spacecraft inertia | J | Diag(2400,2350,3150) | kg-m$^2$ |
| CMG angular momentum | $h_{swr}$ | 50 | N-m-s |
| CMG spin axis inertia | $I_{sw}$ | 0.14 | kg-m$^2$ |
| CMG torque axis inertia | $I_{tw}$ | 0.08 | kg-m$^2$ |
| CMG gimbal axis Inertia | $I_{tg}$ | 0.03 | kg-m$^2$ |
| Max gimbal acceleration | $\ddot{\delta}_{max}$ | 3 | rad/s |
| Reaction Wheel (RW) Inertia | $I_{rw}$ | 0.08 | kg-m$^2$ |
| RW max momentum | $h_{rw}$ | 50 | N-m-s |
| RW max torque output | $T_{max}$ | 0.4 | N-m |

The top level of the simulation can be seen in figure 8. An initial quaternion and body rate are input into the control law, along with the current CMG orientations, wheel rates, and gimbal accelerations, which are used to account for certain components of the torque. The control law outputs a torque request $L_r$ to the steering law, which also takes in CMG torque output capability. It uses this information to determine a wheel acceleration to request from the reaction wheel and gimbal rates to request from the CMGs. The requests are sent to CMG and reaction wheel dynamics blocks to determine the actual torque output, which is affected by motor gains, hardware limitations, and other factors. The resulting torques are added and input to the satellite plant. The plant calculates the spacecraft body's reaction to the torque, finding a new quaternion and body rate for the next step in the simulation.

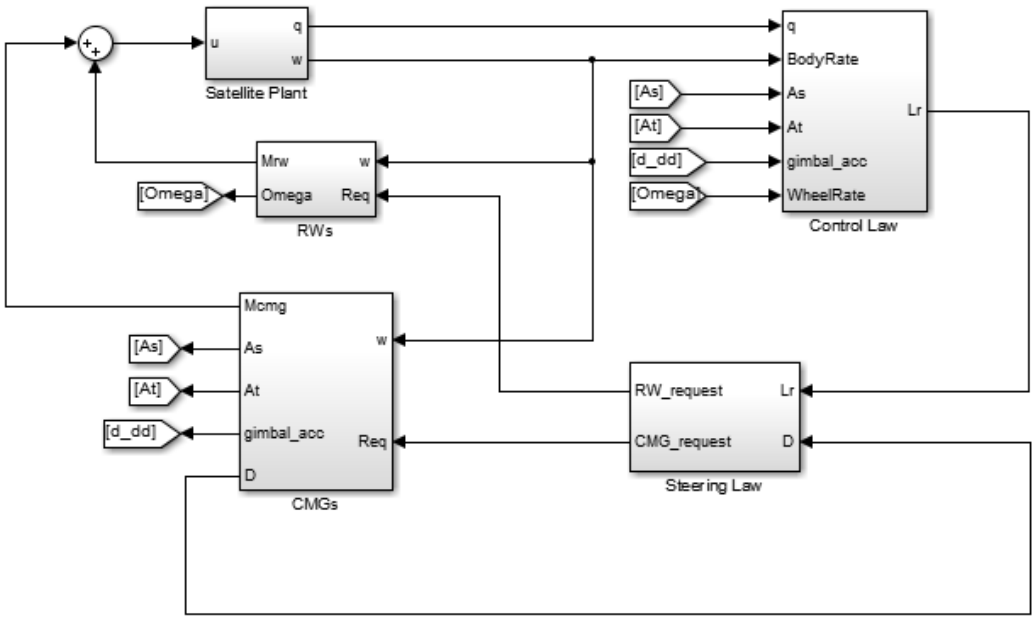


**Figure 8. Top level of the Simulink block diagram.**

The first series of tests were aimed at examining the performance of the control and steering laws for the symmetric maneuverability configuration. The second series of tests examines the performance for the two-axis agility configuration.

### 4.2 Symmetric Maneuverability Configuration

The goal of the symmetric maneuverability configuration was to replace a reaction wheel from a four CMG pyramid configuration with a reaction wheel. This would allow very similar performance while offsetting some of the additional cost, mass, and volume of the CMG system.

As a result, the results of the tests are compared to a typical four CMG pyramid configuration using the same spacecraft and CMGs. A rotated version of this configuration is seen in figure 6 above, with a pyramid angle of 54.74°.

For the 3 CMG setup, a pyramid angle of 68.5° was used. This lower angle allows the reaction wheel to support the CMGs, but most of the torque in the z-axis is still provided by the CMGs.

In the first test, the initial quaternion is [1 0 0 0], and the final quaternion is [0.5 0.5 0.5 0.5], where the first element is the scalar. Initial and final angular body rates are zero, and all gimbal angles start at an initial zero. This offset is representative of a starting angular error of 120°. Figure 9 examines the quaternion difference errors (taken by subtracting the current quaternion from the desired quaternion) for a four CMG system and the mixed system with three CMGs and one reaction wheel.

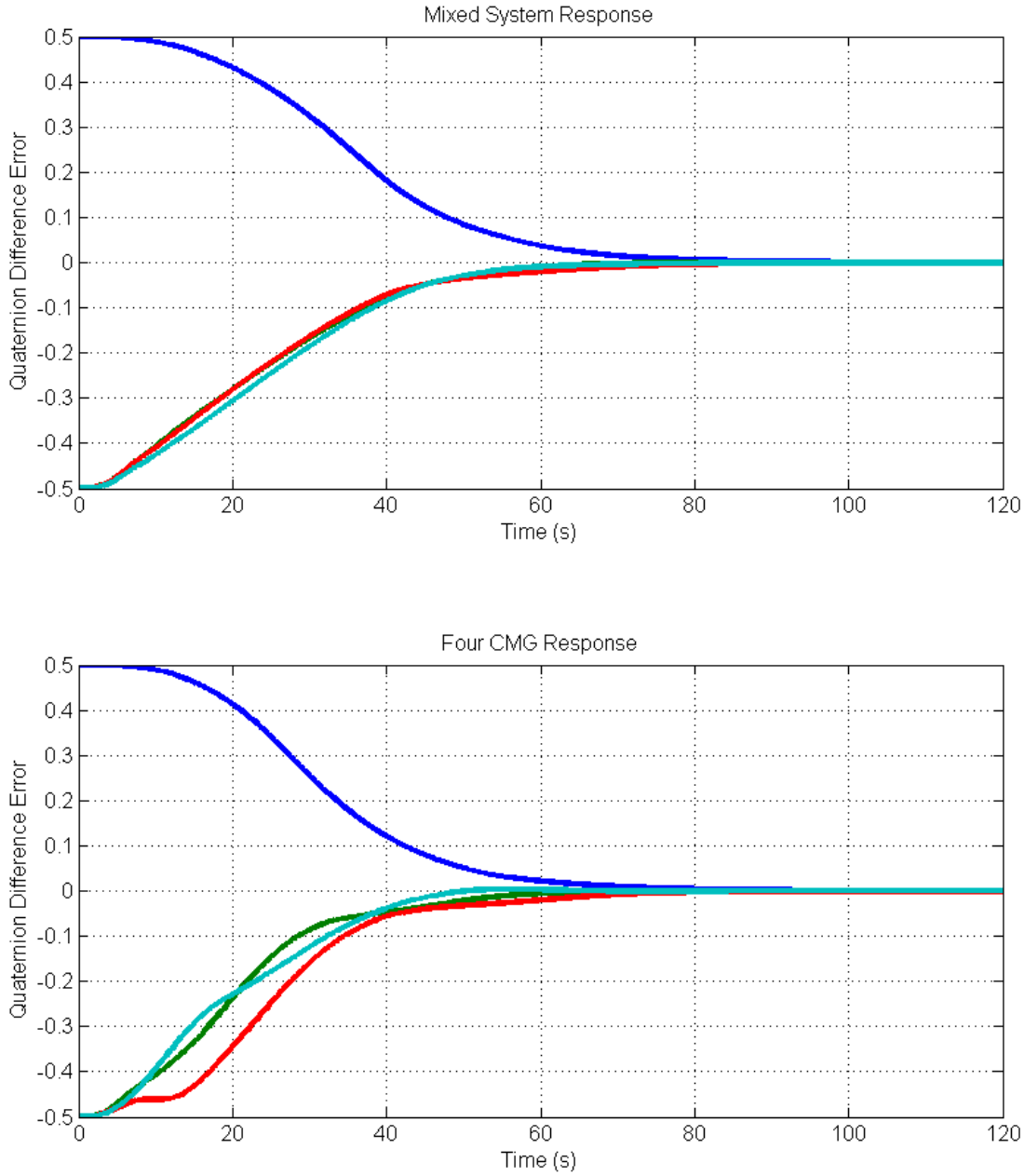


**Figure 9. The quaternion difference error for CMG and mixed systems.** The blue line is the scalar portion of the quaternion, while the red, green, and cyan lines are the vector elements of the quaternion.

Both systems seem to respond well and converge to zero error. The four CMG system does have slightly better performance as may be expected, but overall the responses are very similar. For a more precise comparison, we next examine the angular error – that is the angle between the desired orientation and the current orientation. Additionally, the response of a four reaction wheel system is examined to ensure that the mixed system is a significant improvement over a reaction wheel system. This comparison may be seen in figure 10.

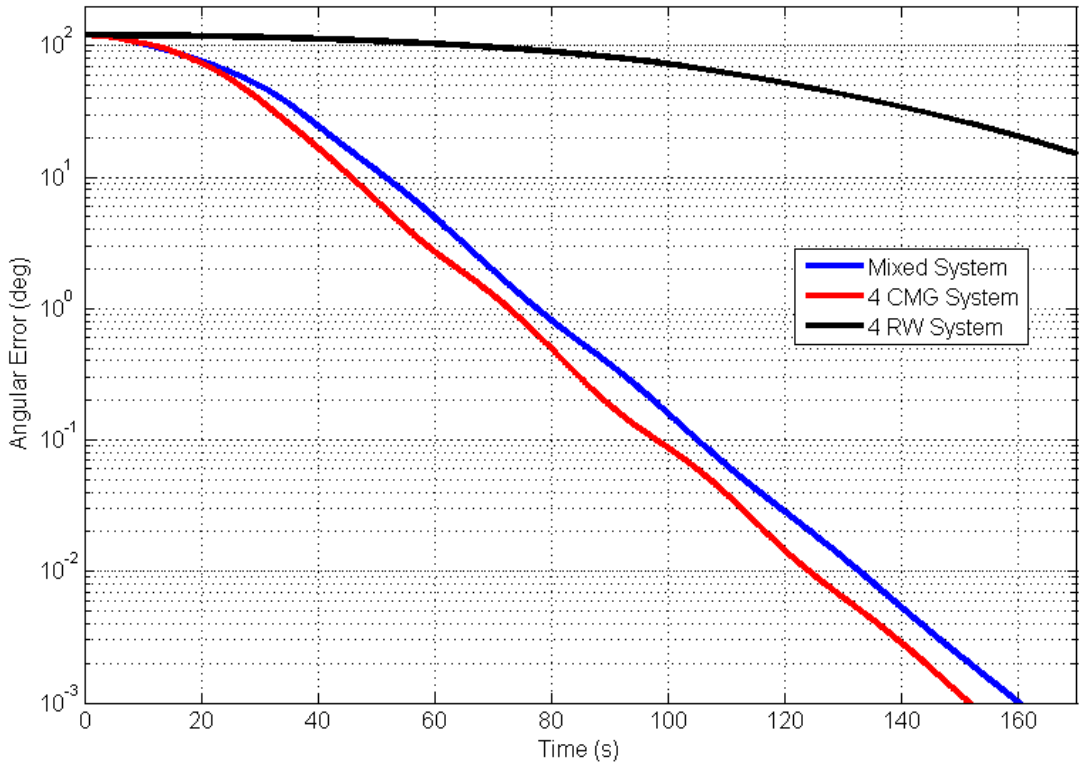


**Figure 10. The angular error response for CMG, reaction wheel (RW) and mixed systems.** The angular error is calculated from the scalar element of the quaternion.

By looking at the angular error over time, it is much easier to note the differences between the responses. Because it has lower torque capability, most of the delay between the four CMG system and the mixed system occurs while the systems are getting up to speed. After that, there is a 5-10 second delay between when the four CMG system reaches a particular accuracy and when the mixed system reaches the same accuracy. For a mission that requires an accuracy of an arcsecond, this would translate to about a 5% increase in transit time.

The response of the mixed system is very close to the response of the four CMG system, particularly in comparison to a reaction wheel system. At the end of the second simulation, the mixed and CMG systems have reached an accuracy of a few arc seconds, while the reaction wheels are still several degrees off from the target. The reaction wheels do not reach this level of accuracy until about 650 seconds from the start of the simulation, taking about four times as long as either the mixed or CMG only systems.

It is important to check the system limitations as well for this large maneuver. The three system limitations focused on are reaction wheel rate, reaction wheel output torque, and gimbal acceleration. All three measures can be seen in figure 11. Reaction wheel speed changes very little relative to its maximum. The reaction wheel torque stays under the maximum extended torque output, and is also under the maximum nominal torque output of 0.2 N-m.[6] The gimbal acceleration also stays within its limitations.[5]

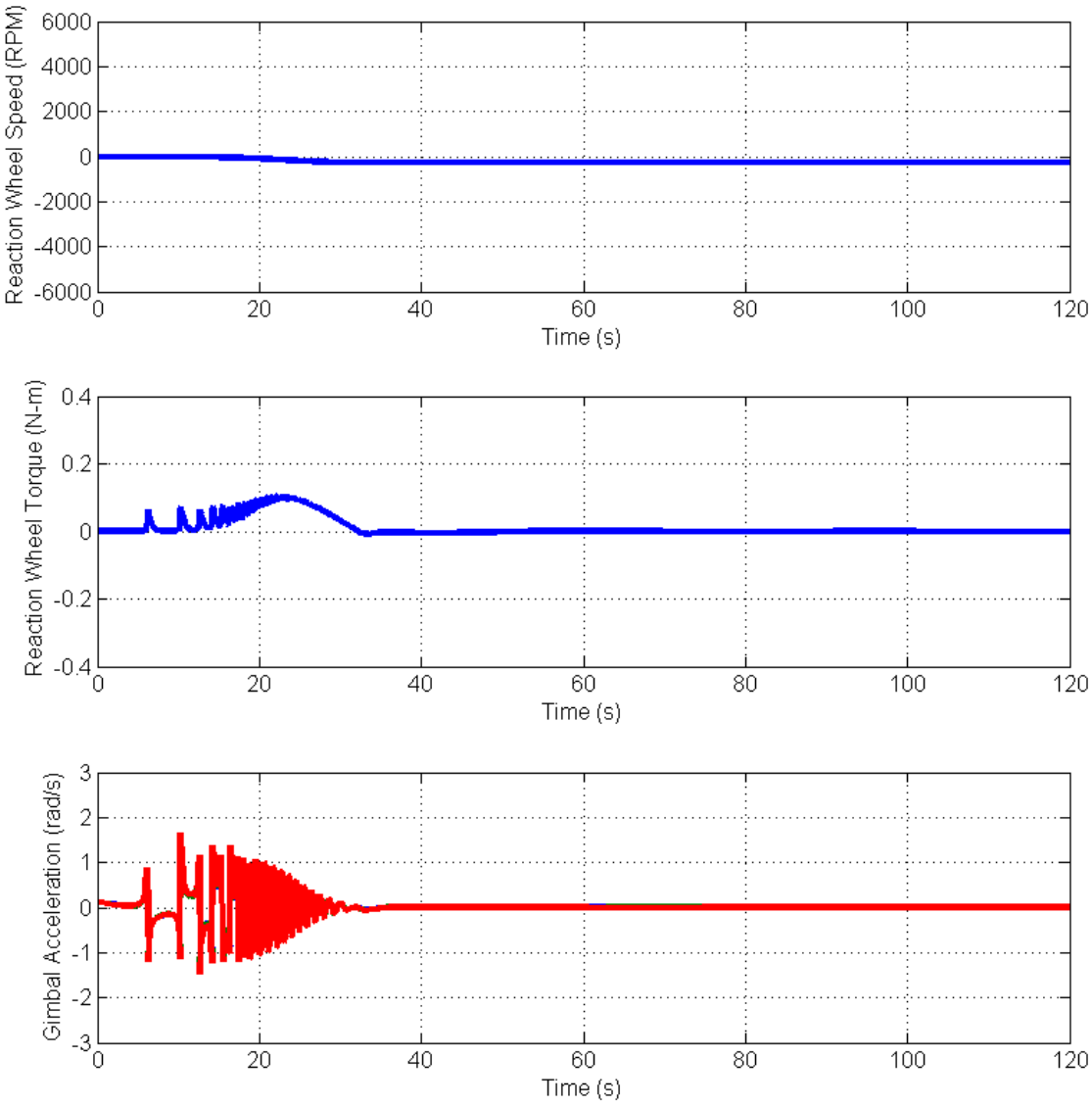


**Figure 11. System limitations during a large maneuver response.** The top and bottom of each diagram represents the maximum that each measurement can output.

In the next series of tests, a smaller initial error is used. The target final quaternion is approximately [0.92 0.18 0.34 0.12] (scalar element first). This corresponds to a 30° yaw, 35° pitch, and 20° roll maneuver, and represents a

total initial angular error of 47°. The first test is under nominal conditions. The angular error is once again used to show the response of the system. This response can be seen in figure 12 below.

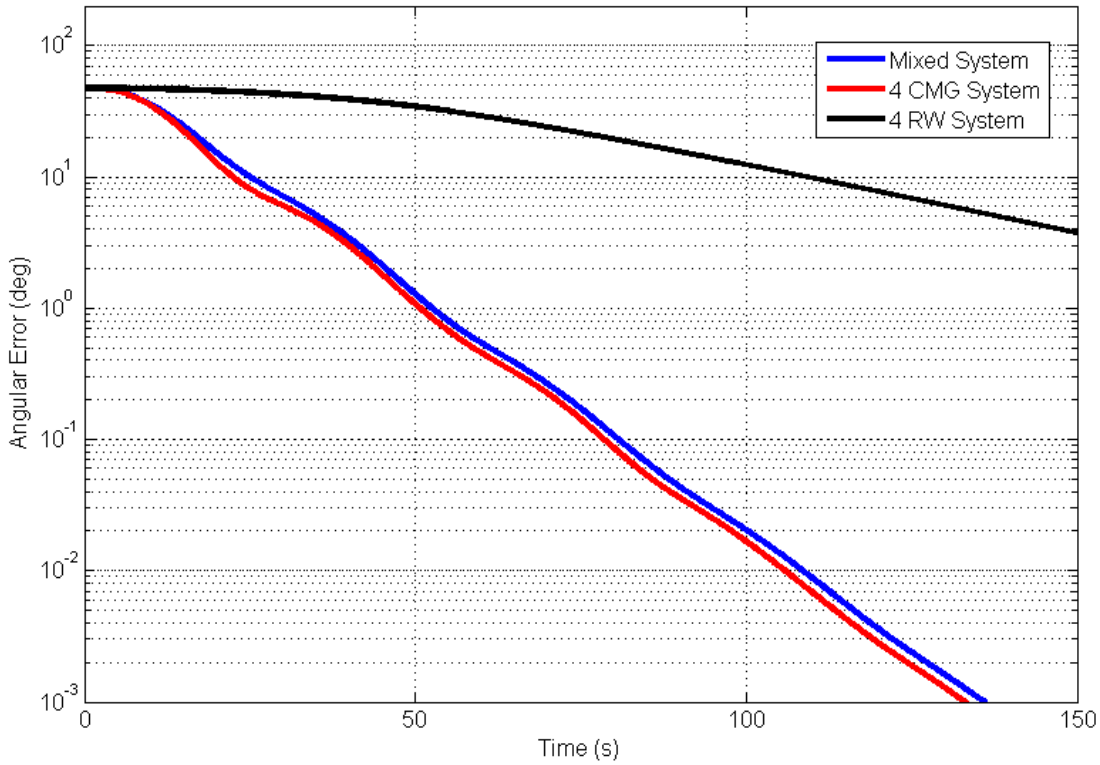


**Figure 12. System responses for the second test maneuver.**

For this smaller maneuver, the response between the mixed system and the CMG system is even closer than in the large maneuver. The delay is reduced to about 2-3 seconds throughout the maneuver past 40 seconds, and the delay is only about 1% at arc second levels of accuracy. The reaction wheel system still takes approximately four times as long to reach the same level of accuracy.

At this point it is important to note the performance of a three CMG system with no reaction wheel to compare the performance of a reduced size CMG system to the mixed system. The reason it is not shown is because the performances in nominal operations are very similar. The delay between the mixed system and the three CMG system for the test in figure 12 was only a few tenths of a second in favor of the mixed system.

This raises the question of why it is favorable to employ a mixed system when a reduced size CMG system performs just as well. The difference occurs in off-nominal conditions. While the steering law allows a system of CMGs to handle some singularities, it still introduces an error into the system. Additionally, some singularities cannot be avoided or escaped. Including a reaction wheel significantly reduces the number of true singularities which may be encountered. Since the reaction wheel torque is lower, it will still encounter reduced performance, but the error introduced will be minimal. An example of a three CMG system encountering a singularity can be seen in figure 13.

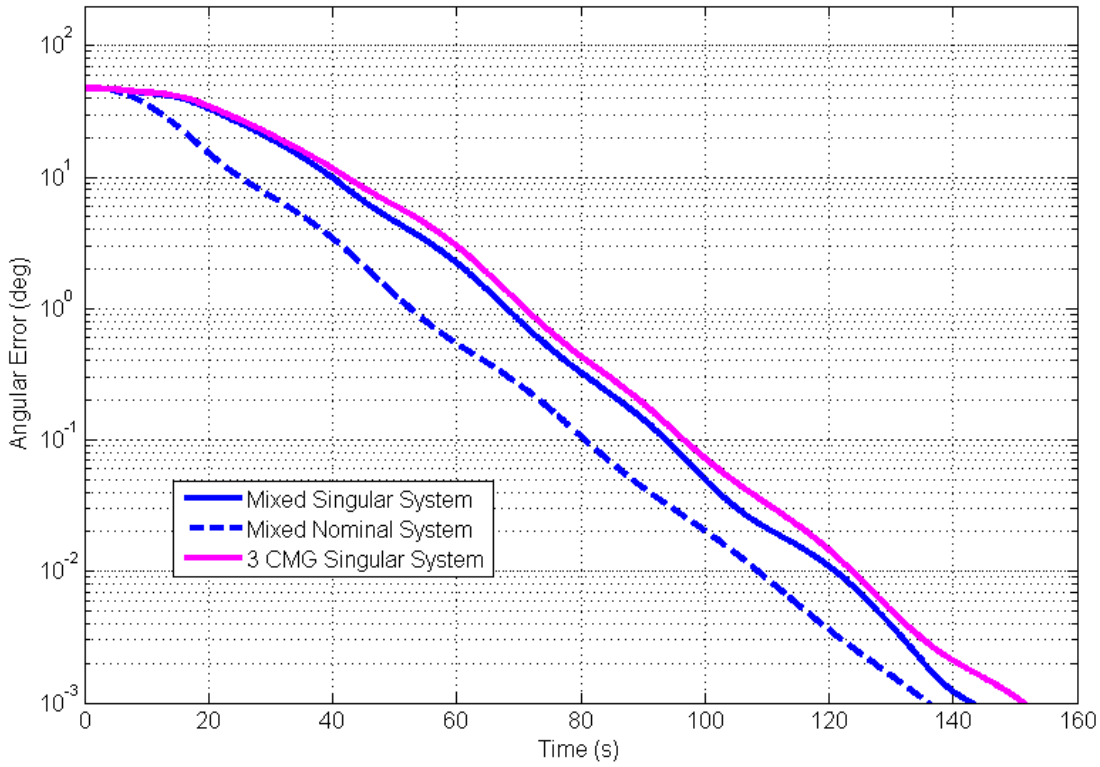


**Figure 13. System response under singular conditions for a mixed system and for a system of three CMGs.**

In the above scenario, the CMGs of both systems are started with gimbal angles of 90°, 90°, and -90°. The four CMG system is not shown, in part because there is no precisely equivalent singularity for the different layout. Most of the time the CMGs will encounter a singular configuration during a maneuver rather than start in one. However, this can be difficult to simulate, so instead the CMGs are started in a singular configuration. The CMGs still have the potential to produce torque in the singular direction, but the initial configuration prevents the system from being able to produce the torque while the gimbals are at those

angles. However, in the mixed system the reaction wheel can still produce torque in the singular direction. Even though the torque produced by the reaction wheel is well below the torque that would normally be produced by the CMGs, it is able to help the CMG break out of the singularity without introducing as much error.

For the mixed system, a delay varying between 7 and 15 seconds is introduced into the system. For the three CMG system, an additional error of 3-9 seconds is added. The error in the systems oscillates quite a bit, but the delay is about 6% for the mixed system and 8% for the CMG system at the arc-second level of accuracy. Some amount of delay occurs even when the system is near a singular configuration, not just in a perfectly singular configuration. As a result, over time this could result in a significant time savings in a mixed system versus a three CMG system.

It is important to note that the delay varies significantly depending on the singular condition. In some singularities, the delay between the mixed and three CMG systems is negligible, and in some cases the delay may be more serious. However, some care must be taken with assigning the scaling for α as seen in equation 20. If it is too low, the CMG system may actually outperform the mixed system. The reason for this is that if the error is introduced is too small, the system may rely primarily on the reaction wheel's low torque, rather than allowing the reaction wheel to help in escape. As a result, it actually can take longer to escape. However, the parameter cannot scale too quickly or unnecessary error may be added to the system.

Another situation that must be accounted for is failure modes. Failure modes are used when one of the devices no longer works. This is the reason why even reliable reaction wheel systems usually have four wheels. By the end of life, it is not uncommon for one of devices to have failed. This is one of the primary reasons why three CMG systems are not typically used. Although CMGs provide torque within a plane, at any given time they can only provide torque in one axis. So if a three CMG system suffers a failure, it is constantly in a singular state.

In the next test, one of the CMGs is “failed” in each system so that it will not produce any torque. Since the configurations are symmetrical, the failure of one should reflect the performance of the failure of any other single device. In this case, for the mixed and 3 CMG system, the gimbal in the z-axis was failed. For the 4-CMG system, the gimbal in the negative y and positive z axes was failed.

In the failed system, the starting gimbal angles are changed. After the loss of one devices, the sum of the angular momenta of the remaining devices no longer adds up to zero. As a result, if the initial angles are not changed (typically performed during momentum dumping) then not only is the momentum envelope reduced by the elimination of a device, but the starting configuration will no longer be in the center of the envelope. So for each configuration, the initial spin axis is recalculated so that the momentum will cancel. The results of the failure test may be seen in figure 14.

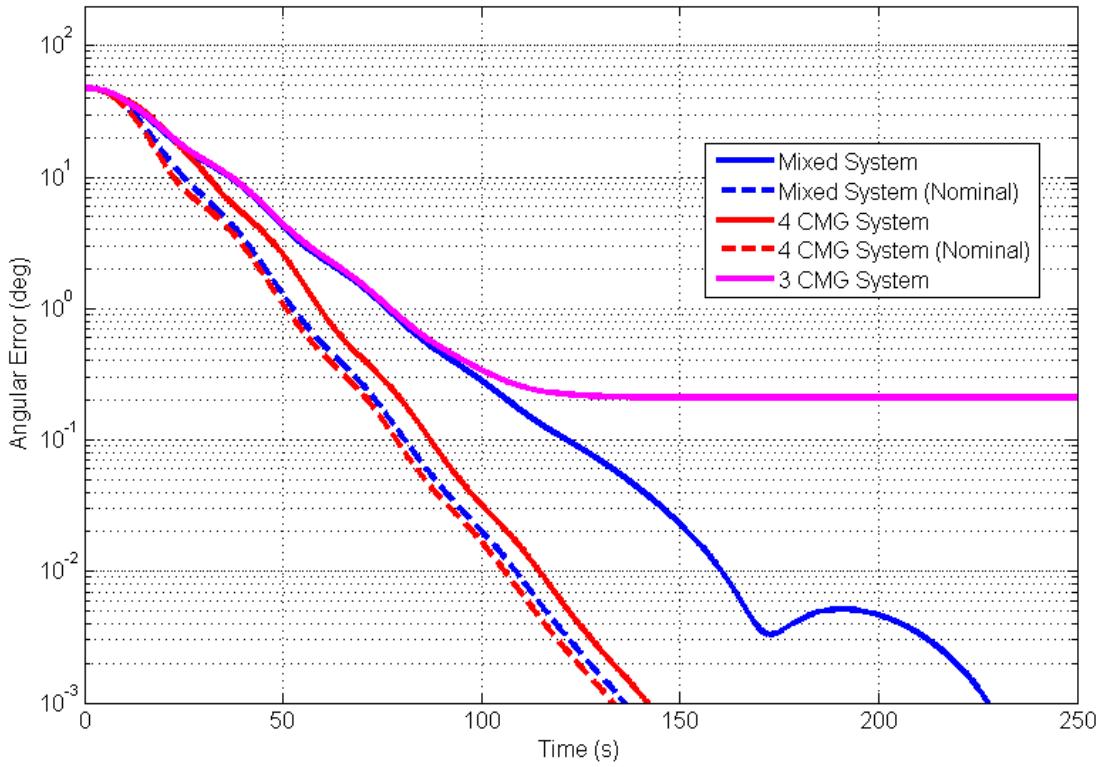


**Figure 14. System response after the failure of a CMG.**

The three CMG system, four CMG system, and mixed system all take a significant hit to performance. Of the three, the four CMG system handles the failure best, and results in similar performance to the three CMG system's nominal performance. The performance is slightly reduced from the nominal three CMG system since the remaining CMGs are not perpendicular. The delay for the four CMG's time to reach arc second accuracy is 8 seconds, or a delay of approximately 6% versus nominal. The mixed system, reduced to two CMGs and one reaction wheel, does not fare quite as well. In this case, the system reaches arc second accuracy with a delay of 91 seconds, a 61% delay versus nominal.

However, this is still an improvement over even the nominal reaction wheel system.

The mixed system does still function properly after a failure, which is not true of the three CMG system. Because the system is constantly in a singular state, error is always introduced into the system by the steering law. This makes it impossible for the CMG system to accurately complete almost any maneuver. The system still moves towards a smaller error however. This may be observed in figure 14 as well. The system initially moves towards the desired orientation but eventually reaches a limit where it cannot get closer. In this case, it is fairly accurate, reaching within 0.2° of the target. However, it is not this accurate in all cases. Depending on the direction, much less accuracy may be achieved. Larger maneuvers in particular are more likely to end with lower accuracy.

To encourage better performance, after a failure some of the gains were also slightly modified. This puts the system at higher risk for hitting limitations, particularly with the additional strain put on the remaining devices. However, the limitations were checked under failure for both the small and large maneuvers, and the devices do not hit their limitations during either of the maneuvers.

The mixed system also has a unique failure mode when the reaction wheel fails. However, the CMG orientation in the symmetric maneuverability mixed system is identical to the orientation of the three CMG system. If the reaction wheel fails, the system essentially becomes the three CMG system whose performance has been described in the previous charts.

A summary of the results of these test are presented in Table 2. The table contains the times required to achieve an accuracy of one arc second for the different system under each test. In all cases, the symmetric maneuverability case was a huge performance improvement over using reaction wheels. The mixed system was also within 6% of the transit time of a four CMG system for normal maneuvers, although after a failure the mixed system took 56% longer. Performance of a three CMG system matched the mixed system for normal maneuvers, but it was slightly outperformed under singular conditions and could not reach the target accuracy after a failure.

**Table 2. Summary of symmetric maneuverability configuration tests.**

| | Mixed | 4 CMG | 3 CMG | Reaction Wheel |
|---|---|---|---|---|
| Large Maneuver | 174 | 165 | 174 | 649 |
| Nominal | 149 | 146 | 149 | 566 |
| Singularity | 158 | - | 161 | - |
| CMG Failure | 240 | 154 | X | - |

### 4.3 Two Axis Agility Configuration

The next series of tests were designed to gauge the performance of a system with a mission to align a payload, sensor, etc. along a particular axis. This is done without regard to the roll angle about that axis so long as the roll rate goes to zero. As before, three CMGs and one reaction wheel are used to control the vehicle. Previously the orientation of the devices relative to the satellite body was not important but in this case it does matter. The sensor boresight axis is aligned with the spin axis of the reaction wheel. This way, the direction with the least torque coincides with the sensor's roll angle.

The first test represents a 30° yaw and 35° pitch maneuver about the sensor axis similar to the previous tests except there is no roll. For comparison, the symmetric maneuverability mixed system's response is included as well. The quaternion for the symmetric maneuverability system is generated from the same 30° yaw and 35° pitch maneuver with no roll. The roll is still commanded but it is essentially commanded to be zero. Since the quaternion difference error is no longer valid for the two axis agility system, the first test results instead show the sensor axis difference error. That is to say it is the sensor axis at a given time minus the desired final sensor axis. This first test can be seen in figure 15.

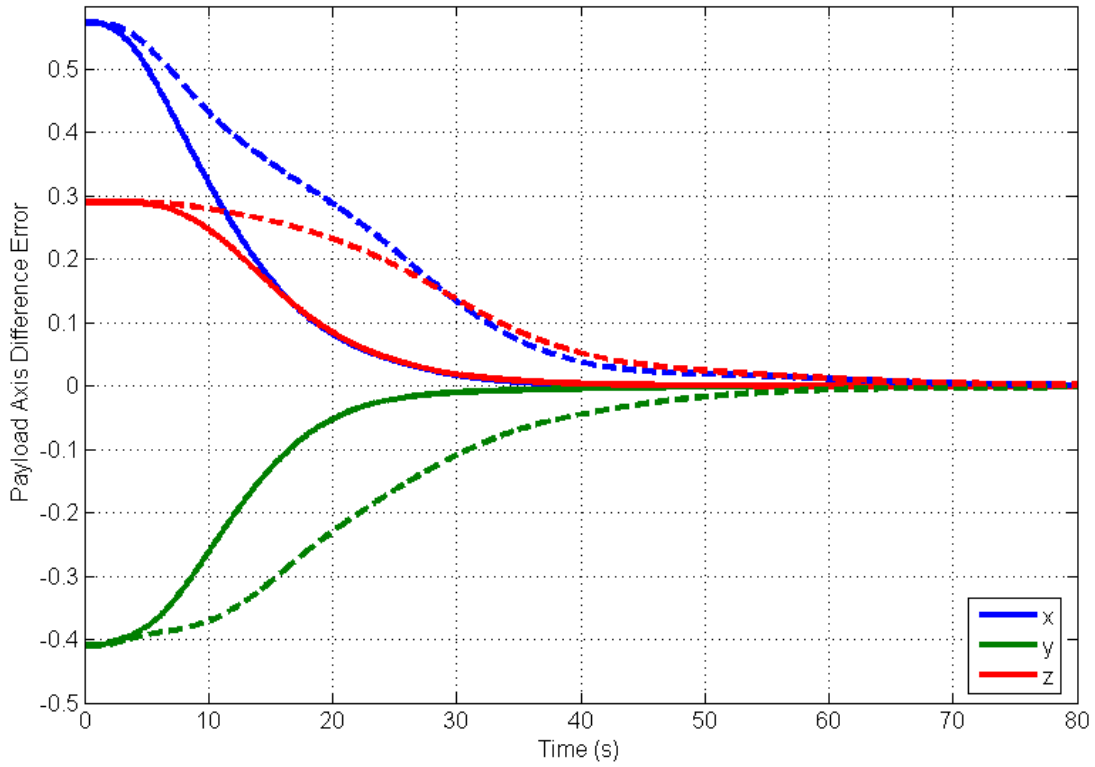


**Figure 15. Sensor axis difference error.** The dotted lines represent the equal torque system's response while the solid lines represent the 2-axis agility system's response.

It is immediately apparent that the two-axis agility system has a faster response than the equal torque system. The most obvious reason for this is that the orientation of the CMGs has been altered to allow more torque in the directions where it is needed – in the pitch and yaw of the sensor axis. In the first trials, this was tested without changing the control law, but the performance was not as greatly improved. Even though no roll is requested in the symmetric manueverability system's control law, a zero angle is commanded. As a result,

the roll is not allowed to stray from its initial angle throughout the maneuver, requiring a notable amount of torque to be used about the roll axis. For reference, the roll angle of the 2-axis agility system is shown in figure 16.

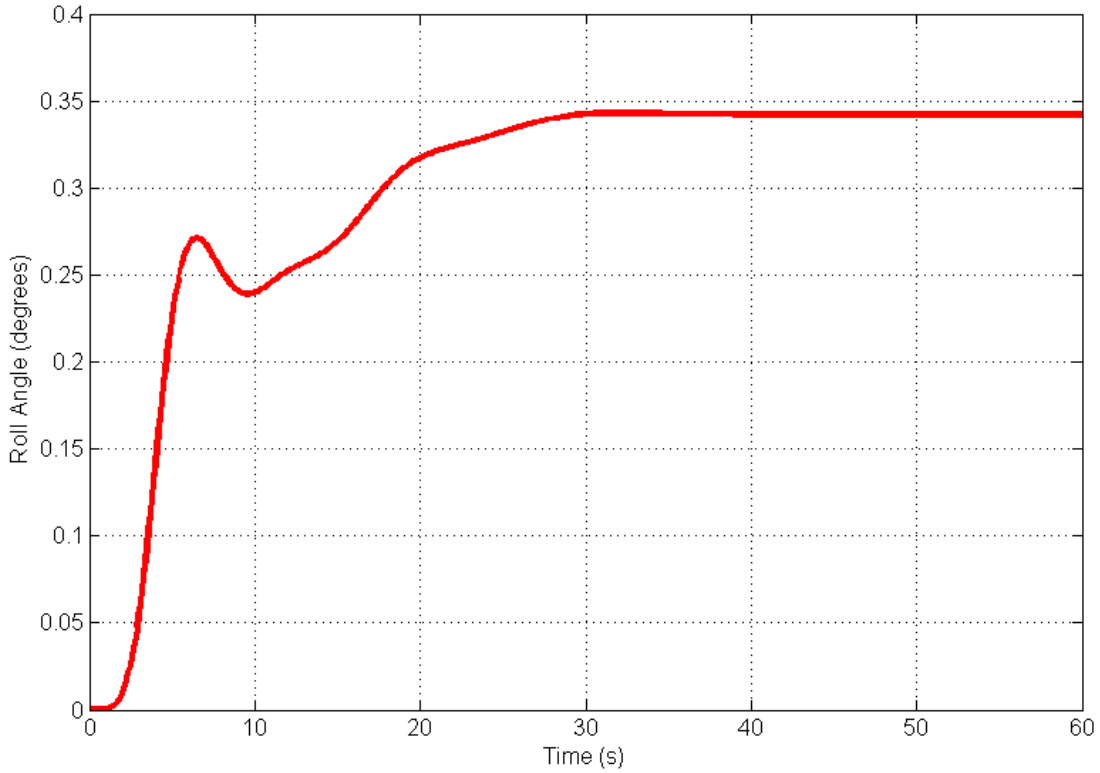


**Figure 16. Roll angle about the sensor axis during the maneuver**.

The roll angle is certainly not constant during the maneuver, although the angle change is fairly small, less than 0.4° at the end. The fact that this is small may be convenient depending on the mission. For example, if there is an ideal roll angle for the solar panels, then that roll angle can be set before maneuvering begins and will not wander too far. For a cosine power loss on the solar panels, a

0.4° angle only translates to a 0.002% power loss. This could add up over the course of several maneuvers (depending on the sequence) but may be corrected during momentum dumping.

It's also important to check that the roll rate is converging to zero since this is impossible to tell from the angular position error. The angular rates of the satellite during the maneuver can be seen in figure 17. As expected, the sensor axis stays close and converges to zero angular velocity.

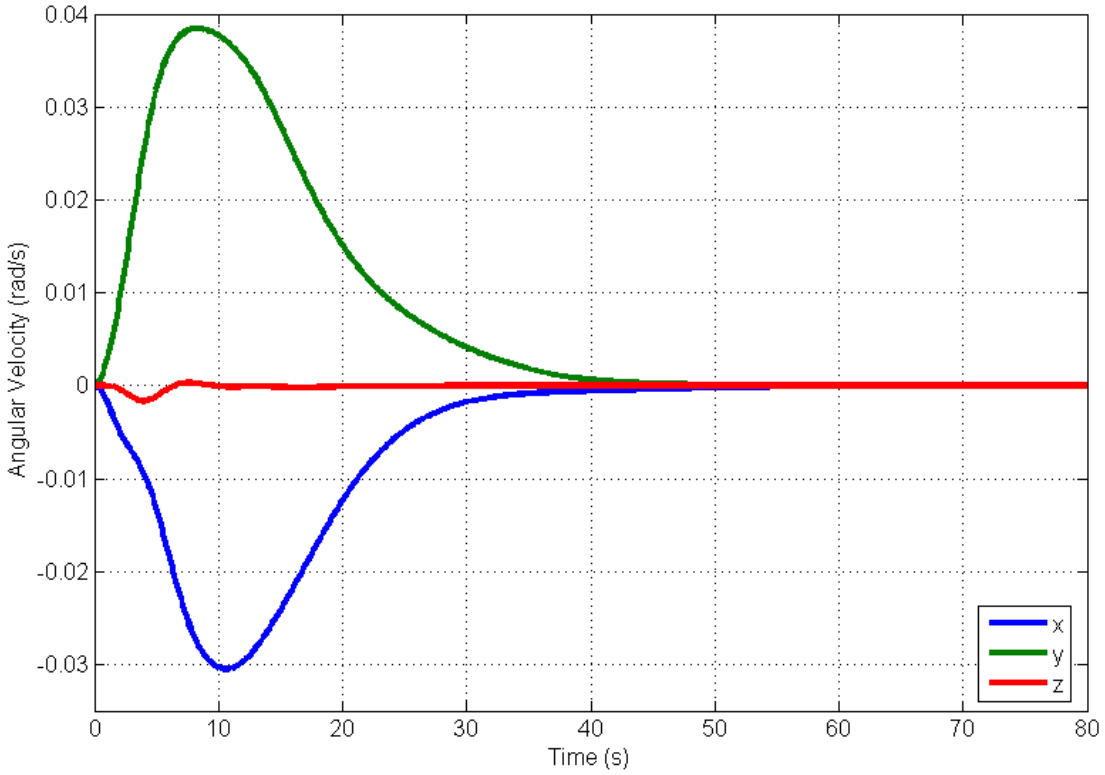


**Figure 17. Angular body rates during the maneuver**. For this test, the sensor axis was aligned with the z-axis for clarity. As a result, the z-axis angular velocity barely strays from zero.

The same maneuver can be seen again in figure 18, which uses the angle error instead. Instead of the quaternion error angle, as was used before, this is the actual angle between the current and desired sensor axis. For comparison, the symmetric maneuverability system and 4 CMG system are also included. Additionally, a modified version of the 4 CMG system is included. It uses the same control law as the 2-axis agility system, but the hardware configuration is the same.

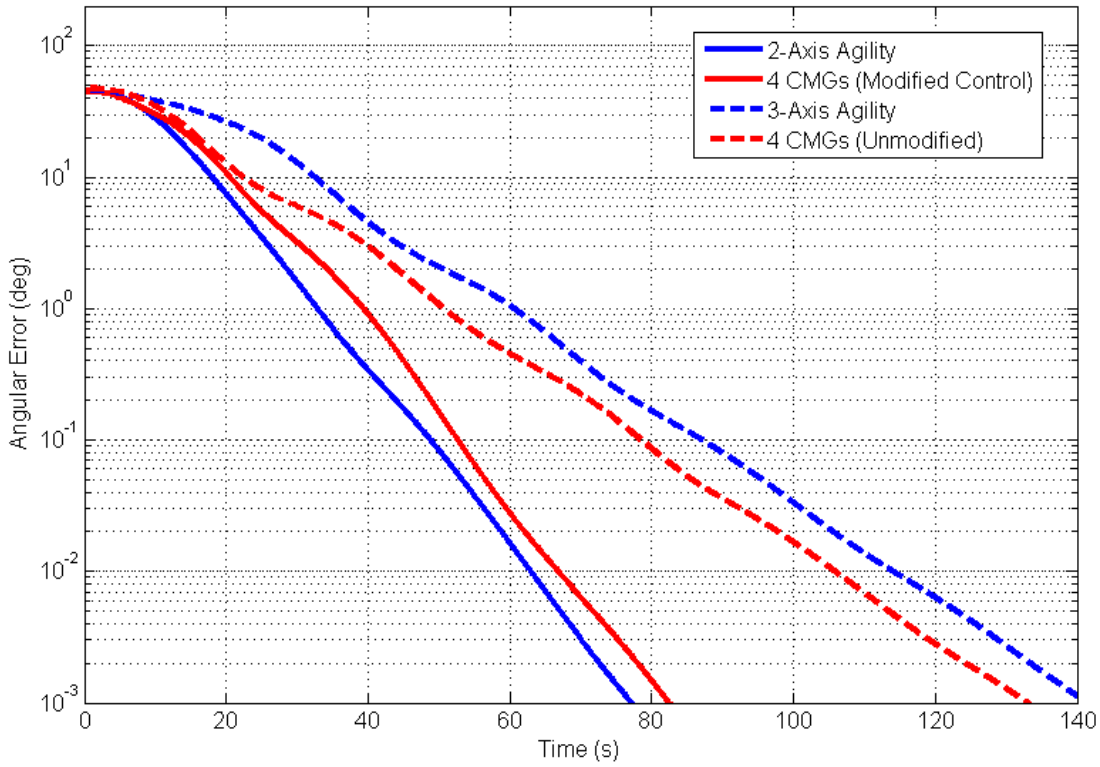


**Figure 18. Angular error for the mixed systems, modified and unmodified four CMG systems.**

It is clear that the combination of altering the control law and the configuration of the hardware produces far better results than the symmetric maneuverability and unmodified four CMG system. It takes both systems almost twice as long to reach arc-second accuracy. In this case, the mixed system actually performs slightly better than the 4-CMG system despite having one less CMG. The reason for this is the orientation of the CMGs in the mixed system. The inclusion of the reaction wheel allows the CMGs to be oriented with a lower pyramid angle, and therefore each individual CMG has more torque available in the x and y axes. As a result, it produces slightly more torque in the needed axes even though the 4 CMG system can produce more torque overall.

The 4-CMG system could be modified so that the angle is lowered and it can produce more torque in the x-y plane (across the sensor axis). However, in doing so, it would lose its symmetric momentum envelope. This may be acceptable in some contexts, but doing so will generally require the angular momentum of all wheels increased to cover the needs of the sensor axis. Otherwise the momentum will have to be dumped more often, which delays normal usage of the satellite and may increase fuel usage. By contrast, looking at equations 26 and 28, the pyramid angle can be lowered in the mixed system by increasing the size of the reaction wheel without increasing the size of the CMGs. The system will have an increased momentum envelope which retains its symmetry. While this has limitations, it is a much cheaper way of increasing the response of the system without compromising the angular momentum envelope.

Next, failure modes are examined. Once again, the failure of the reaction wheel does not notably affect the performance, although this significantly reduces the amount of angular momentum that can be absorbed. As before, it also is at high risk if a CMG fails as well, and is at increased risk of singularities. This is not as big of a concern since one axis is not commanded for position, but it can still affect performance. For a CMG failure, figure 19 shows the angular error for the mixed system and the CMG system.

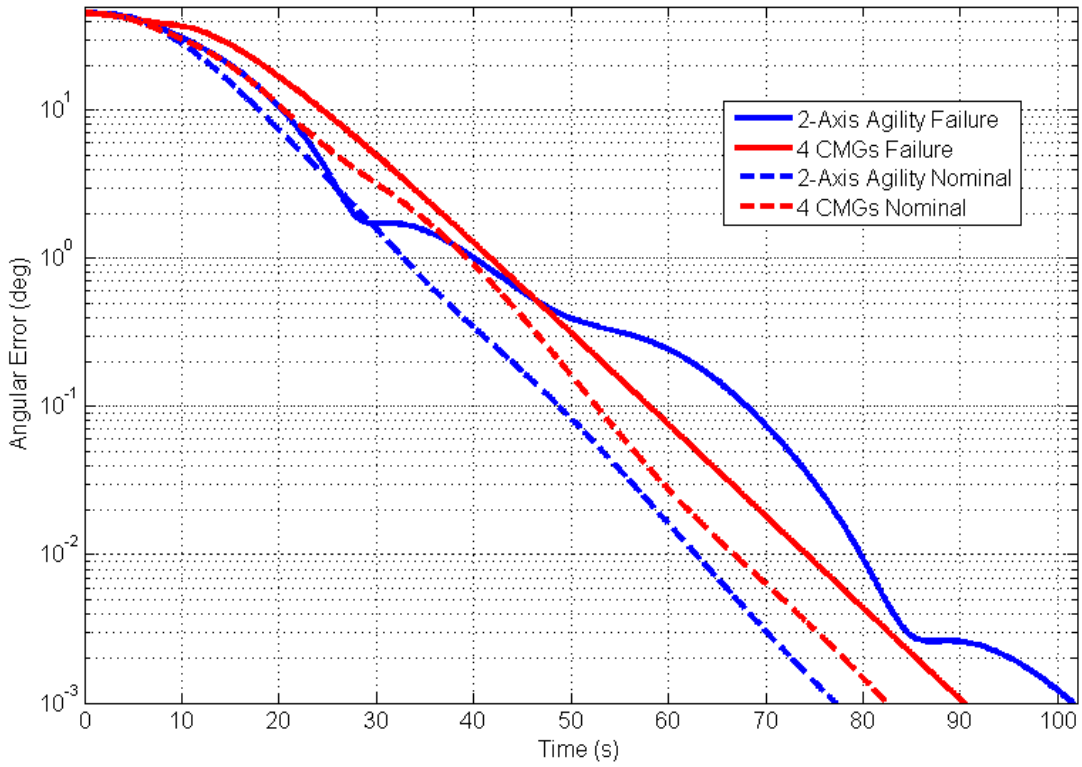


**Figure 19. Performance of two systems nominally and after CMG failure.**

After a failure, both systems suffer in performance, but the mixed system is more harshly affected – enough so that it no longer outperforms the four CMG system. At first, the mixed system seems to perform quite well, but eventually it begins to struggle with singularities and is surpassed by the four CMG system.

Even after a CMG failure, the 2-axis agility system performs better than the systems where zero roll is commanded. The 2-axis agility mixed system also is not as harshly affected by the CMG failure as the symmetric maneuverability system was. The symmetric maneuverability mixed system experienced an increased delay of a minute and a half, about 67% longer, while the delay for the 2-axis agility system is 24 seconds, or about 28% longer.

Under a CMG failure, the roll angle drifts more than it does nominally. However, if necessary this can be controlled to some extent. This is done by adjusting the gain for the angular rate control in the direction of the sensor axis. An example of this can be seen in figure 20. For the modified gain presented in the figure, the increase in maneuver time was about 10 seconds for a reduction of 1° in the final angle. The roll angle can be further decreased, but the cost in terms of delay will quickly rise.

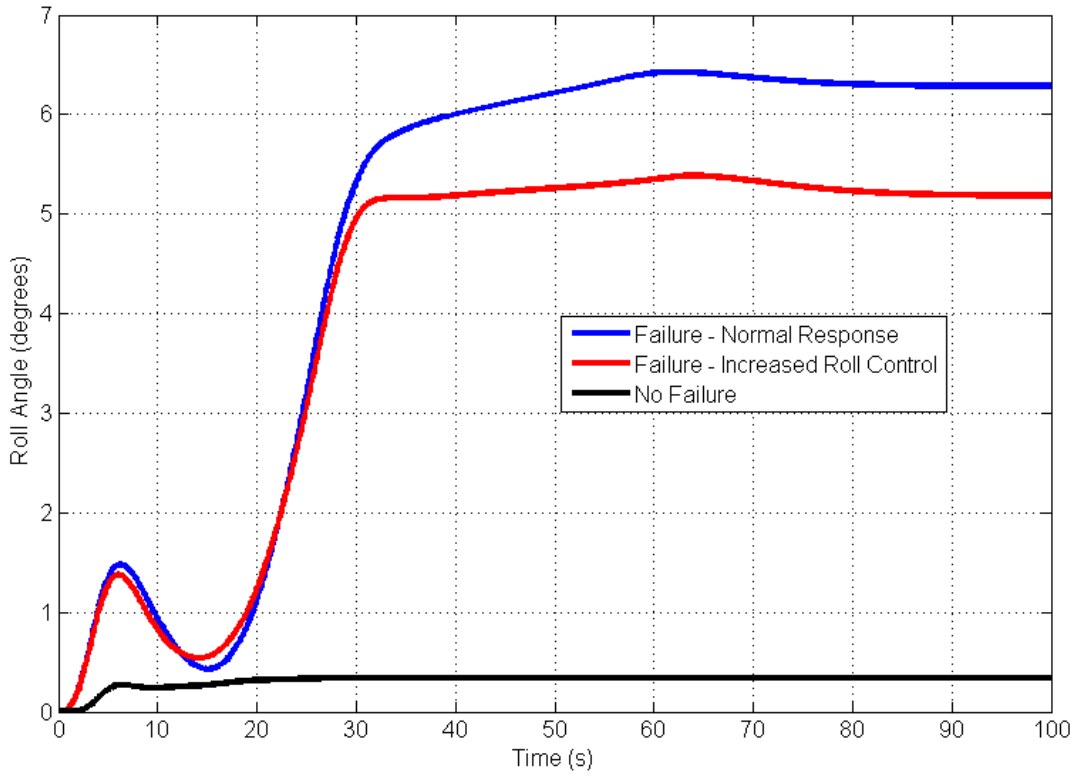


**Figure 20. Roll angle drift with a CMG failure vs. nominal.**

The full results of the 2-axis agility configuration testing may be seen in table 3 below. For the nominal case, both the two axis agility and modified CMG system were far superior to the unmodified control law systems. For this setup however, the 2-axis agility case actually outperformed the modified four CMG case slightly. The roll angle, allowed to drift, changed by about 0.35° for this maneuver of about 45°. The 2-axis agility case was more strongly affected by a CMG failure, just as the symmetric maneuverability case was. After a failure, the four CMG case outperforms the 2-axis agility case. However, the 2-axis agility case fares much better than the other mixed system, suffering an increased

delay of about 28% instead of the symmetric maneuverability's 61%. After a CMG failure, the roll angle drifts significantly more, by about 6.3°. If necessary, this angle may be reduced at the cost of reduced performance.

**Table 3. Summary of 2-axis agility configuration tests.**

| | 2-axis agility | Modified 4 CMG | Symmetric Maneuverability | 4 CMG |
|---|---|---|---|---|
| Nominal | 85 | 89 | 149 | 146 |
| CMG Failure | 109 | 98 | 240 | 154 |

# 5. Conclusion

## 5.1 Summary

In this thesis, the performance of a mixed system of CMGs and reaction wheels was evaluated. The purpose of this mixed system was to show that a system with both reaction wheels and control moment gyros could achieve similar performance to an all CMG system. Replacing a CMG with a reaction wheel would cut cost and mass while still using known and tested equipment. A summary of the derivation of the equations of motion for momentum exchange devices was presented.

Two control schemes were reviewed. One offers a symmetric maneuverability similar to the traditional CMG pyramid configuration, while the other is based on requirements of agility in only two axes. The performance of the symmetric maneuverability system was only slightly reduced from the four CMG system and far better than a four reaction wheel system. The system performed well against singularities and is able to compensate for both CMG and reaction wheel failures, unlike a three CMG system.

The two-axis agility system performed better than either the symmetric maneuverability configuration or the four CMG system under either control law. It also outperformed the other mixed system as well as the unmodified four CMG system after a CMG failure. While a four CMG system may be able to achieve superior performance, it would be at the cost of reduced momentum absorption capability in one axis.

## 5.2 Future Work

Several courses could be taken to advance the work presented in this paper. This paper primarily examined the replacement of a single CMG with a reaction wheel. For certain missions, it may be possible to replace two CMGs with reaction wheels, particularly if only one axis needs agility, for example in the cross ground track. This would be considerably more difficult. Ideally, the two CMGs would be parallel so that they would not need to rely on the low torque reaction wheels to cancel out torque in the wrong direction. Relying on the reaction wheels for this purpose could seriously limit the system's agility. However, if the two CMGs are aligned, then the momentum envelope could only be equal in each axis if the two reaction wheels also aligned perpendicular to the CMG torque plane. If this were the case however, a failure of one CMG would cripple the system. As a result, careful configuration of the hardware will be required.

A single CMG with three reaction wheels would be even more difficult to manage. A single CMG cannot maintain torque in a single axis and the reaction wheels cannot produce enough torque to keep up with torque produced by the CMG in the wrong direction.

The simulation in this project was entirely software simulation. Both reaction wheels and CMGs are frequently used on spacecraft. However, it still would be wise to test these configurations on hardware before any implementation. Although Cal Poly does have a spacecraft simulator, it contains

only reaction wheels and no CMGs and therefore could not be used to confirm the computer simulations.

A full simulation over a longer period of time, including external torques, would allow the momentum envelope of each configuration and scenario to be tested as well. This would be particularly important for the symmetric maneuverability configuration, which does not have symmetric angular momentum envelope. It would also be useful for comparing the performance of a four CMG system tailored to a two axis agility problem, since it would likely encounter momentum absorption difficulties. This is of course dependent on further factors which influence external torques, such as surface area that are mission dependent. For this reason and also for the sake of optimizing the hardware setup, gains, and other parameters, it is important to consider the mission and satellite when deciding if the mixed control scheme is best.

Finally, the singularities and the effect of the reaction wheel on them should be further studied. The performance under singular conditions was highly dependent on the scaling used for the error. It may be that the reaction wheel would be more helpful in a singular avoidance type steering law, since it could be used to aid in null motion. The reaction wheel does reduce error introduced in singular escape laws, but this can become dangerous if the reaction wheels are too heavily relied on. In future projects, this alternative steering law would be recommended.

# REFERENCES

[1]Wertz, J., *Space Mission Engineering: The New SMAD*, Microcosm Press, Hawthorne CA, 2011. p. 580

[2]Votel, R., and Sinclair, D., "A Comparison of CMGs and Reaction Wheels for Small Earth Observing Satellites," AIAA/USU Small Satellite Conference, August 2012.

[3]Yoon, H., "Spacecraft Attitude and Power Control Using Variable Speed Control Moment Gyros," PhD Dissertation, School of Aerospace Engineering, Georgia Institute of Technology, Atlanta, GA, 2004.

[4]Hall, C., Tsiotras, P., and Shen, H., "Tracking Rigid Body Motion Using Thrusters and Momentum Wheels," AIAA/AAS Astrodynamics Conference, August 1998.

[5]Honeywell, "M50 Control Moment Gyroscope," Specification Sheet, N61-0096-000-001, Phoenix, AZ, January 2006.

[6]Honeywell, "Constellation Series Reaction Wheels," Specification Sheet, N61-0045-001-001, Phoenix, AZ, December 2003.

[7]Kramer, H., "SPOT-6 and SPOT-7 Commercial Imaging Constellation," eoPortal, August 2014.

[8]Skelton, C., "Mixed Control Moment Gyro and Momentum Wheel Attitude Control Strategies," Master's Thesis, Virginia Polytechnic State University, Blacksburg, Virginia, November 2003.

[9]Roithmayr, C., “Dynamics and Control of Attitude, Power, and Momentum for a Spacecraft Using Flywheels and Control Moment Gyroscopes,” NASA TP-2003-212178, April 2003.

[10]Richie, D., Lappas, V., and Prassinos, G., “A practical small satellite variable-speed control moment gyroscope for combined energy storage and attitude control,” *Acta Astronautica*, Vol. 65, May 2009, pp. 1745-1764.

[11]Leve, F., “Development of the Spacecraft Orientation Buoyancy Experimental Kiosk,” Master’s Thesis, University of Florida, May 2009.

[12]Chen, X., and Steyn, W., “Robust Combined Eigenaxis Slew Manoeuvre,” Guidance, Navigation, and Control Conference and Exhibit, August 1999.

[13]Ye, D., Sun, Y., and Wu, S., “Hybrid Thrusters and Reaction Wheels Strategy for Large Angle Rapid Reorientation with High Precision,” *Acta Astronautica*, Vol. 77, August-September 2012, pp. 149-155.

[14]Lappas, V., Steyn, W., and Underwood, C., “Control Moment Gyro Gimbal Angle Compensation using Magnetic Control During External Disturbances,” Guidance, Navigation, and Control Conference and Exhibit, August 2001.

[15]Leve, F., “Novel Steering and Control Algorithms for Single-Gimbal Control Moment Gyroscopes,” PhD Dissertation, University of Florida, Gainesville, FL, 2010.

[16]Paradiso, J., “A Highly Adaptable Steering/Selection Procedure for Combined CMG/RCS Spacecraft Control – Detailed Report,” Charles Stark Draper Laboratory, CSDL-R-1835, Cambridge, MA, March 1986.

[17]Ford, K., and Hall, C., “Singular Direction Avoidance Steering for Control-Moment Gyros,” *Journal of Guidance, Control, and Dynamics*, Vol. 23, No. 4, 2000, pp. 648-656.

[18]Kurokawa, H., “A Geometric Study of Single Gimbal Control Moment Gyros,” TR 175, Mechanical Engineering Lab., Tsukuba, Ibaraki, Japan, Jan. 1998.

[19]Markley, F., Reynolds, R., Liu, F., and Lebsock, K., “Maximum Torque and Momentum Envelopes for Reaction Wheel Arrays,” *Journal of Guidance, Control, and Dynamics*, Vol. 33, No. 5, 2010, pp. 1606-1614.

[20]Paradiso, J., “A Search-Based Approach to Steering Single Gimballed CMGs,” Charles Stark Draper Laboratory, CSDL-R-2261, Cambridge, MA, August 1991.